Title

Cannabinoid receptor-1 controls human mucosal-type mast cell degranulation and maturation *in situ*

Koji Sugawara, MD, PhD[1,2], Nóra Zákány, MS[1,3*], Torsten Hundt, Dipl.Pharm[1*], Vladimir Emelianov, MD, PhD[1#], Daisuke Tsuruta, MD, PhD[2], Christian Schäfer, MD[4], Jennifer E. Kloepper, DVM[1], Tamás Bíró, MD, PhD[3] and Ralf Paus, MD[1,5]

[1]Department of Dermatology, University of Luebeck, Luebeck, Germany

[2]Department of Dermatology, Osaka City University Graduate School of Medicine, Osaka, Japan

[3]Department of Physiology, DE-MTA "Lendület" Cellular Physiology Research Group, MHSC, RCMM, University of Debrecen, Debrecen, Hungary

[4]E.N.T. Clinic Luebeck, Schuesselbuden, Luebeck, Germany

[5]Institute of Inflammation and Repair, University of Manchester, M13 9PT Manchester, United Kingdom

**These authors are contributed equally*

[#]*current address:* Department of Dermatology, Boston University School of Medicine, Boston, MA

Corresponding author: Koji Sugawara, MD/PhD

Department of Dermatology, Osaka City University Graduate School of Medicine,
1-4-3, Asahimachi, Abeno-ku, Osaka, 545-8585, Japan

Telephone: 0081-6-6645-3826, Fax: 0081-6-6645-3828

Email: kojilaminin@yahoo.co.jp

Declaration of all sources of funding: This study was supported in part by a grant from Deutsche Forschungsgemeinschaft (DFG, GRK 1722) to RP. All authors have declared that they have no conflict of interest.

Key Messages

1. The degranulation and maturation of human mucosal-type mast cells is controlled by cannabinoid receptor (CB)-1. This is clinically relevant in the context of the aetiopathology of nasal polyps.

2. CB1 may be a new target in the management of diseases in human bronchial mucosa including allergic rhinitis and bronchial asthma.

Capsule summary

Human nasal polyp organ-culture offers a clinically relevant model for investigating human mucosal-type mast cells (hMMC) *in situ*. We show that hMMC activation and maturation from resident progenitors is constitutively controlled by endocannabinoids *via* CB1.

Key words Nasal polyp, mucosa, organ culture, endocannabinoid, cannabinoid receptor, mast cell, SCF, c-Kit, tryptase, chymase

Abbreviations:

MC mast cell

NP nasal polyp

CB cannabinoid receptor

ECS endocannabinoid system

SCF stem cell factor

ABSTRACT

Background: Since many chronic inflammatory and allergic disorders are intimately linked to excessive mast cell (MC) number and activation, it is clinically important to understand the physiological mechanisms preventing excess MC accumulation/degranulation in normal human tissues.

Objective: Since endocannabinoids are increasingly recognized as neuroendocrine regulators of MC biology, we investigated how cannabinoid 1 (CB1) receptor-signaling affects human mucosal-type MCs (hMMCs).

Methods: Using organ-cultured nasal polyps (NP) as a surrogate tissue for human bronchial mucosa, we investigated by quantitative (immuno)histomorphometry and ultrastructurally how CB1 stimulation, inhibition or knock-down impacts hMMCs biology.

Results: Kit+ hMMCs express functional CB1 *in situ*. Blockade of CB1-signaling (using specific CB1 antagonist, AM 251, or CB1 gene knock-down) enhanced hMMCs degranulation and increased their total number without affecting their proliferation *in situ*. This suggests that inhibiting CB1-signaling induces hMMC maturation from resident progenitor cells within human mucosal stroma. hMMCs maturation was induced at least in part *via* up-regulating stem cell factor (SCF) production. Both the prototypic endocannabinoid, anandamide, and the CB1-selective agonist, arachidonyl-2-chloroethylamide, effectively counteracted secretagogue-triggered excessive hMMCs degranulation.

Conclusions: The current serum-free NP organ-culture model allows physiologically and clinically relevant insights into the biology and pharmacological responses of primary hMMCs *in situ*. In human airway mucosa, hMMCs activation and maturation

are subject to a potent inhibitory endocannabinoid tone *via* CB1 stimulation. This invites one to target the endocannabinoid system in human airway mucosa as a novel strategy in the future management of allergic diseases.

While the central role of human mucosal-type mast cells (hMMCs) in respiratory diseases, including allergic rhinitis and asthma, is well-appreciated,[1,2] most research on hMMCs relies on isolated cells obtained during bronchial lavage or cell lines.[3,4] Instead, studies that examine and manipulate *primary* hMMCs within their natural tissue habitat, the respiratory tract mucosa, are scarce.[5-7] However, it is crucial to study hMMC *in situ*, rather than in isolated cell culture, since MC functions (including activation, degranulation, maturation, proliferation and apoptosis) are critically influenced by their immediate tissue environment; vice versa, MCs greatly impact on the tissue they reside in, namely in the airways.[8-12] For such *in situ* studies of hMMCs, nasal polyps (NPs) have long offered a very attractive, yet still regrettably under-appreciated assay options for clinically relevant *in situ*-MC research in the human system.[5,6]

NPs represent polypoidal masses that arise mainly from nasal and paranasal mucous membranes and are frequently associated with allergic rhinitis and other “atopic” diseases.[13,14] Since nasal mucosa forms one functional continuum with the upper respiratory tract mucosa,[15,16] the organ culture of NPs can serve as an easily accessible, well-defined, and abundantly available surrogate tissue for – much less readily obtainable – bronchial mucosa and its hMMC populations.[5,6] Moreover, hMMCs also play an important role in the pathogenesis of NP formation as such [2,5,17-19] so that MC research in organ-cultured NPs simultaneously allows one to investigate one of the most common clinical problems of upper respiratory tract medicine.

Previous human NP organ culture models,[3,20] are limited by relatively rapid NP decay and/or the presence of bovine serum in the culture medium, require special matrix

support systems, and/or have not systematically addressed key MC biology questions, such as the physiological controls of hMMC maturation and activation *in situ*. Therefore, we aimed to develop a very simple, serum-free organ culture system that i) prolongs NP tissue viability *in vitro*, and ii) permits the quantitatively study of key MC research parameters *in situ*, and iii) permits instructive functional and mechanistic studies, including pharmacological manipulations and gene-knock-down, of primary hMMCs *in situ*.

As a potentially interesting system that may control hMMC functions, we turned to the endocannabinoid system (ECS). The ECS is composed of cannabinoid receptors (CBs), their endogenous ligands and enzymes responsible for endocannabinoid synthesis and degradation.[21-25] Components of the ECS are increasingly recognized as important neuroendocrine regulator of MC biology.[21,26-28] Notably, we have recently reported in this journal that the ECS limits excessive human *skin* MC activation and maturation *via* CB1-mediated signaling *in situ*.[29] However, the role of CB-mediated signaling in hMMCs still remains largely unknown (see supplementary text **S1**). Therefore, we investigated the effects of CB1 stimulation/blockade on hMMCs biology within organ-cultured human nasal mucosa.

METHODS

Human nasal polyp (NP) organ culture

Human NP samples were obtained from 5 males and 2 females (aged: 23-80, average: 41.4) undergoing elective surgery for nasal obstruction (polypectomy). Human tissue collection and handling was performed according to Helsinki guidelines,

with Institutional Research Ethics approval (University of Luebeck) and written informed consent. Freshly isolated NPs were cut into small pieces (6 x 6 x 6 -10 x 10 x 10 mm) and maintained in supplemented serum-free William's E medium.[29-32] NPs were first incubated overnight to adapt to culture conditions after which the medium was replaced and vehicle or test substances were added. For the organ culture with substance P, compound 48/80 and corticotropin-releasing hormone (CRH), NPs were first treated with N-arachidonoylethanolamine (anandamide, AEA, 30 μM) or arachidonyl-2-chloroethylamide (ACEA, 30 μM) for 1 day after the overnight incubation. Then the NPs were treated with substance P (10^{-10} M) or compound 48/80 (10 μg/ml)[29] or CRH (10^{-7} M)[31] in the combination with AEA or ACEA for additional 1 day. Following NP organ-culture for the indicated time, tissue was processed for cryo- or paraffin sections and histochemistry, immunohistochemistry, or transmission electron microscopy. Data from test and control groups within one set of experiments were generated by using only NPs from the same patient.

CB1 knock-down

CB1 silencing in organ-cultured human NPs was performed using the previously reported method.[29]

Immunohistochemistry/Immunofluorescence microscopy

For the detection of CB1, stem cell factor (SCF), Kit, high affinity IgE receptor (FcεRI)α, tryptase and chymase immunohistochemistry, paraffin embedded sections were used. For the immunofluorescence study for Kit, CB1 and SCF, cryo-embedded

sections were also used (for details, see this article's Methods section in the Online Repository).

hMMCs were defined as "degranulated" when more than 5 histochemically or immunohistologically detectable MCs granules could clearly be observed outside the MC membrane (see representative degranulated MC in Fig. E1A).[29,31]

Quantitative immunohistomorphometry and transmission electron microscopy (TEM)

Quantitative immunohistomorphometry of the observed immunoreactivity patterns in defined reference areas were assessed according to the previously described principles [29-32] using the ImageJ software (National Institutes of Health, Bethesda, MD). TEM was done as previously reported.[29]

Statistical Analysis

Data were analyzed using either the Mann-Whitney *U*-test for unpaired samples or 1-way ANOVA, Bonferroni's multiple comparison test, using Prism 4.0 software (GraphPad Prism Program, GraphPad, San Diego, CA). *p* values <0.05 were regarded as significant. All data in the Figure are expressed as mean + SEM. * P<0.05, ** P<0.01, *** P<0.001, comparing the indicated experimental groups.

RESULTS

Human NPs can be organ-cultured for at least 7 days

First, we adapted the long-term organ culture human skin[30,31] to the organ culture of human NPs, using supplemented, serum-free William's E medium. This simple and cost-efficient assay preserved NP architecture for at least 7 days (later time points were not examined). Even at day 7 after culture initiation, the NP tissue architecture and cellularity were reasonably well-preserved, and even mucosal cilia in the NP epithelium as well as blood vessels and collagen fibers of the NP stroma (lamina propria) were partially conserved (Fig 1A and B).

After a temporary decline subsequent to the trauma of tissue dissection, at day 7, cell proliferation in the NP epithelium quickly recovered, and had reached again initial day 0 levels (Fig 1C). In contrast, cell proliferation within the NP lamina propria remained stable throughout the examined organ culture period (Fig 1D). Although intermittently increased stroma cell apoptosis was observed at day 3 (Fig 1E), general tissue decay parameters (% of apoptotic [TUNEL+] cells, LDH release) also had stabilized by day 7 (Fig 1E, F and E1B). However, with increasing organ-culture time, the NP stroma became slowly more edematous (Fig. 1A). This needs to be accounted for when calculating cell numbers per reference area in NP organ-culture.

hMMCs are detectable histochemically and immunohistochemically in NP organ culture

Multiple fully granulated (Fig 2A) or degranulated (Fig 2B) hMMC could be detected histochemically at all examined time points of NP organ culture. For this, Leder's esterase [Fig 2A] or Giemsa [Fig 2A] or alkaline Giemsa histochemistry [Fig E1C] provided optimal cell visualization and morphological detail. Since the FcεRIα+ is not only expressed on hMMC (Fig 2A), but also e.g. on Langerhans cells, basophils,

platelets, eosinophils, monocytes and dendritic cells,[33,34] FcεRIα+ proved to be a less instructive marker of mature hMMCs in NPs compared to classical MC histochemistry (toluidine blue, Leder's esterase, Giemsa and alkaline Giemsa histochemistry, Fig 2A and Fig E1C) on the one hand, or tryptase (Fig 2A and B) or chymase immunohistochemistry (Fig 2A) respectively on the other.

Most Kit+ cells in human NP stroma clearly represented hMMCs as indicated by co-expression of FcεRIα, and the majority of hMMCs in NP stroma was of the tryptase+/chymase- subtype (for details, see supplementary text S2 and Figs. E1D**,** E1E**).**

Furthermore, to assess whether the number of hMMCs within the lamina propria varied during organ culture, tryptase or Kit (CD117)[29,31] immunohistochemistry was performed. The number of tryptase+ hMMCs in the lamina propria was stable during NP organ culture (Fig E1F), while that of Kit+ hMMCs increased (Fig. E1G). In view of the slowly progressing NP edema (Fig. 1A), the number of tryptase+ hMMCs may actually have increased during organ-culture, while the observed numeric increase Kit+ hMMCs probably even exceeds the absolute values measured here.

The percentage of cells positive for tryptase (which demarcates mature MCs) and Kit+ cells (which demarcates both immature MC and MC progenitors[29,35,36]) increased until day 7 (Figs. 2C and D). However, there was no significant increase in Kit+ cells proliferation (Ki67) (Fig E2A). This suggests that during NP organ-culture new, mature hMMCs differentiate *in loco* from resident progenitor cells. Interestingly, immunoreactivity for the Kit ligand, SCF, was still detectable in the NP epithelium at day 7 (Fig 2E). The continued presence of this key MC growth factor[1,2,8,29] may

explain in part why hMMCs can be preserved in NPs during prolonged organ-culture without serum or exogenous growth factors, and why there is hMMC maturation from (preexisting) resident MC progenitors.

hMMCs express functional CB1

Next, we employed this simple, optimized, and serum-free, clinically relevant NP organ culture assay to investigate whether a new regulatory principle of human MCs that we had previously identified in human connective tissue-type MCs[29] also applies to hMMC *in situ*. Namely, we had shown that the ECS limits both, the degranulation of mature connective tissue-type MCs and the local maturation of these MC from resident progenitor cells in human skin *in situ via* CB1 stimulation.[29] However, the role of the ECS in hMMC biology *in situ* remains obscure, and whether a similar CB1-mediated “inhibitory tone” is also established in the control of primary hMMC activation and maturation within normal respiratory tract mucosa is completely unknown.

Therefore, we first checked, whether Kit+ hMMCs in the NP lamina propria express CB1. This is the case (Fig 3A). Furthermore, stimulation with the highly CB1-selective ligand, Tocrifluor T1117[29] demonstrated functional binding activity of these receptor proteins with CB1-like IR for a cognate, specific ligand (Fig 3B).

CB1 inhibition induces hMMCs degranulation and increases their number

Just as in human skin MCs,[29] the CB1-specific synthetic agonist, arachidonyl-2-chloroethylamide (ACEA)[29,37] or the non-selective endocannabinoid

CB1 agonist, anandamide (AEA),[10,29,32] did not significantly increase the number of tryptase+ hMMC in human NPs (counted as number of tyrptase+ cells per visual field [Fig. E2B and C] and as %positive cells per total number of cell nuclei [Fig. 3C, D and E, Fig. E3]). hMMC degranulation was also unaffected by these CB1 agonists (Fig 3F and G, Fig. E4).

In contrast, the specific CB1 antagonist, AM251,[29,32] significantly increased both, the number (Fig. E2B and C, Fig. 3D and E, Fig. E3) and the degranulation of tryptase+ hMMCs *in situ* (Fig. 3C, F and G, Fig. E4). This was abrogated by the co-administration with ACEA or AEA (Fig 3D-G, Fig. E3 and 4). Increased hMMCs degranulation by CB1 specific antagonist was independently confirmed by high resolution light microscopy of alkaline Giemsa histochemistry (Fig. E1C and E2D) and by transmission electron microscopy (Fig. E2E).

Since MCs degranulation typically induces mucosal edema,[38,39] we next investigated the impact of the CB1 antagonist on NP edema. Indeed, AM251 decreased the cellularity (i.e. number of total nuclei/mm^2) in the NP lamina propria compared to the control group (Fig. E6A and B) and thus NP edema, likely as a result as CB1 blockade-induced MC degranulation.

CB1 inhibition promotes the maturation of resident hMMC progenitors in NP stroma

Intriguingly, AM251 also significantly increased the number and the percentage of Kit+ hMMCs *in situ* (Fig. E2G, Fig. 4A, Fig. E5, left panel]). However, just as in human skin MCs *in situ*,[29] proliferation (Fig. 4B) or apoptosis (Fig. 4C) of hMMC did not change significantly after pharmacological CB1 blockade. Therefore, the increased number of

detectable mature hMMCs can only have arisen from resident progenitor cells. Since human nasal mucosa, besides tryptase+ hMMCs (Fig. 3D and E, Fig. E3), exhibits many chymase+ MCs,[40] it is interesting to note that CB1 blockade also increased the number and the percentage of chymase+ hMMCs *in situ* (Fig. 4D, E2H, E5, right panel).

Importantly, the impact of CB1 stimulation/blockade on hMMCs degranulation and numbers *in situ* was highly consistent between distinct NP assays derived from 4 different patients (Fig. E3-5). For human tissue organ culture standards, where data variability - even between tissue samples derived from the same patient - can be substantial, the observed CB1 agonists/antagonist effects on hMMCs degranulation and on the percentage of Kit+, tryptase+ and chymase+ cells *in situ* are unusually robust and we—reproducible. This underscores the usefulness of the current human NP organ culture assay as a hMMC research model.

CB1 blockade increases the number of hMMCs within the NP epithelium

hMMCs, which migrate towards and into the NP epithelium, may play an important role in NPs pathogenesis.[41 42] Therefore, we asked whether CB1 stimulation/blockade also affects the location of hMMC within the NP. Interestingly, already after a single day of AM251 treatment the number of tryptase+ *intraepithelial* MCs was significantly increased compared to controls (Fig. 4E and F). This was partially abrogated by co-administration of the CB agonist, ACEA (Fig. 4F). This suggests that signaling through CB1, which is also expressed on NP epithelial cells (Fig. 5A see untreated skin), impacts on hMMC migration into the NP epithelium.

296 ***The CB1 gene can be silenced in organ-cultured human NPs***

297 Next, CB1 gene silencing was attempted, using the same protocol we had previously
298 described for human hair follicles.[29] Effective epithelial and mesenchymal CB1
299 knock-down was demonstrated by a significant down-regulation of CB1
300 immunoreactivity by 40% in the epithelium (Fig 5A and B), and on CB1+ stromal cells
301 (Fig 5A and C) of organ-cultured NPs. Similar to the effects of pharmacological CB1
302 blockade (Fig. 3D-G and Fig. 4A, D and E), CB1 gene silencing significantly increased
303 the percentage of tryptase+ hMMCs in the lamina propria (Fig 5D) and stimulated their
304 degranulation (Fig 5E). These data independently confirm that CB1 blockade induces
305 hMMC maturation from *resident* progenitor cells and induces hMMC degranulation *in*
306 *situ* not only in human skin mesenchyme[29], but also in human respiratory tract
307 mucosa.

308

309 ***Endocannabinoids inhibit excessive activation of hMMCs via CB1***

310 Excessive MCs degranulation and numbers in human mucosa play a key role in the
311 pathogenesis and clinical phenotype of major allergic diseases of the respiratory
312 tract.[1,7,33] Therefore, we then asked whether CB1 stimulation counteracts the
313 MCs-activating effects of two classical endogenous MCs secretagogues that play a
314 key role in MC-dependent neurogenic airway inflammation: substance P[29,43-47] and
315 corticotropin-releasing hormone (CRH).[31,48] In addition, we examined the exogenous
316 standard MC secretagogue, compound 48/80.[29]

317 Quantitative tryptase-immunohistomorphometry demonstrated that both, the potent
318 endocannabinoid AEA and the CB1-specific agonist, ACEA, inhibited the

degranulation-promoting effects of substance P (Fig. 6A), CRH (Fig. 6B) and compound 48/80 (Fig. 6C). Thus, exactly as in human skin MCs,[29] CB1 stimulation effectively counteracts excessive MC activation in normal human mucosa *in situ*.

CB1 regulates stem cell factor expression by the NP epithelium

Since increased SCF production (along with enhanced number and degranulation of MCs) has been reported in the nasal epithelium of patients with allergy,[49] we asked whether CB1 inhibition also affects SCF expression in human nasal mucosa *in situ*.

Faint SCF-like immunoreactivity was detected within the NP epithelium at day 7 (Fig 2G). Compared to the vehicle control group (Fig 7A, left photo), CB1 inhibition by AM251 significantly increased SCF-like immunoreactivity in the NP epithelium after only 1 day of NP organ culture (Fig 7A, right image and Fig 7B). Furthermore, the up-regulation of the number of tryptase+ hMMCs by pharmacological CB1 blockade (AM251) was completely abrogated by neutralizing SCF (Fig 7C). This suggests that enhanced hMMCs maturation by CB1 blockade in NPs *in situ* is mediated at least in part *via* up-regulation of SCF expression and increased SCF secretion by the NP epithelium.

DISCUSSION

Our data provide the first evidence that normal hMMCs utilize CB1-mediated signaling to limit not only their degranulation, but also their maturation from resident progenitor MC cells *in situ*. The observed effects of pharmacological or transcriptional CB1 blockade may be induced not only directly *via* CB1 receptors on the cell membrane,

but also indirectly by up-regulating SCF-production within the NP epithelium *in situ*. These results underscore the key role of the ECS in human MC physiology, and confirm the importance of CB1-mediated signaling as an endogenous, “tonic” control system that avoids excessive MC maturation and degranulation, which we had previously identified for human connective tissue-type MCs in human skin.[29]

This clinically and biologically important confirmation-of-concept in a different tissue system (human airway mucosa versus skin) is complemented by additional novel insights:

1. The current study closes an important gap in the human MC biology literature by clarifying the effect of CB1-mediated signaling on normal primary hMMCs *in situ*.

2. CB1 signaling (both, *via* directly impacting on MCs membrane receptor and indirectly *via* controlling epithelial SCF secretion) has a universal regulatory effect not only on human connective tissue-type, but also on hMMCs *in situ*, and is no peculiarity of the hair follicle-associated MCs we had investigated before.[29]

3. Our demonstration that CB1 blockade increases the number of *intraepithelial* MCs in NPs (Fig. 4E and F) shows that CB1 signaling also regulates hMMC location and migration.

4. We show that serum-free human NP organ culture provides a very instructive, clinically relevant model system that generates robust and well-reproducible data for investigating the biology of hMMCs and their response to pharmacological manipulation *in situ*. However, apoptosis as well as increased hMMC maturation from resident progenitor cells do occur in this *ex vivo* system. Therefore, even though adult primary hMMCs do operate within their natural tissue habitat in this assay, NP organ culture as such impacts MC biology *in situ* and cannot be entirely equated with the

physiological *in vivo* situation. Yet, the translational relevance of human NP organ culture for clinical respiratory medicine surely exceeds that of mainstream mucosal MC research that relies on mouse *in vivo* models and human cell lines.

5. Our assay system also allows instructive studies on how MC secretagogues and MC degranulation inhibitors impact the physiology and pathology of human airway mucosa *in situ*.

Systematic exploitation of this NP assay may also shed new light on the as yet unclear role of hMMCs in NP pathogenesis.[41,42,49] Moreover, our findings raise the possibility that insufficient CB1-mediated signaling (e.g. in the epithelium) triggers excessive, SCF-mediated influx of hMMC into the epithelium of nasal mucosa. This may be relevant not only to NP pathogenesis, but also to other hMMCs-dependent human airway pathologies. If the ECS indeed operates (e.g. *via* CB1 signaling) as a safeguard system against excessive epithelial SCF production and secretion (to limit undesired MC maturation, activation, and migration into/towards the epithelium), the future management of allergic upper airway diseases could profit from re-establishing effective CB1-mediated signaling (e.g., up-regulation of intramucosal endocannabinoid levels by inhibition of their degradation by FAAH inhibitors[23-25]).

We were surprised to find fewer Kit+ MCs than tryptase+ or chymase+ MCs (Fig. 2C and D, Fig. E5, patients 1 and 2), since Kit is often interpreted as a universal marker for detecting both immature and mature MCs.[50] However, only 70-90% of tryptase+ cells in human samples from stomach, colon, and breast tissue reportedly are Kit+.[51] In line with this, the percentage of Kit+ MCs in the lamina propria of NPs from some patients was lower than that of tryptase+ or chymase+ hMMCs (Fig. E3 and 5). Moreover, besides MCs, basophils (which are Kit-negative,[52] yet can be a prominent

feature of NP immunopathology[53]) all can be tryptase-positive.[54] Taken together, this may explain the lower number of Kit+ MCs compared to that of tryptase+ or chymase+ MCs in organ-cultured NPs and shows that Kit has inherent limitations as a “universal” marker for hMMCs, also in human NPs.

Fully in line with our previous results obtained from human skin MCs,[26] CB1 blockade significantly increased the number of total Kit+ hMMCs without modifying their proliferation or apoptosis in organ cultured NPs (Fig. 4B and C). Although Kit demarcates both immature and mature MCs,[50] there are no selective markers for immature hMMC progenitors, and some trytase+ hMMC do not even express Kit *in situ*.[51] In fact, Kit-negative MC progenitors have previously been reported in human peripheral blood,[55] and their existence has been deduced from morphometric data in the connective tissue sheath of human scalp HFs.[29,31] This renders it likely that Kit- MC progenitors also exist in human NPs.

In the NPs of some patients, the number of Kit+ MCs was even lower than that of tryptase+ or chymase+ MCs (Fig. E3 and 5). Therefore, the number of MC progenitors in NPs cannot be reliably estimated by simply subtracting the number of tryptase+ MC from that of Kit+ MCs. However, the percentage of Kit+ MCs increased significantly during organ culture (Fig. 2D). Moreover, there were no indications of significant CB1 antagonist-induced proliferation of Kit+ progenitor cells. Instead, the number of mature hMMCs (i.e. hMMCs expressing the differentiation-associated proteins tryptase and chymase) rose significantly. Since the isolated NP samples had no connection to the bone marrow or vasculature, these unequivocal findings can only be explained by the differentiation of at least some resident MC progenitor cells into mature MCs.

That co-administration of CB1 agonists counteracted the CB1 blockade-induced excessive hMMC maturation (Fig. 3D and E, Fig. 4A and D) supports a key role for CB1 in controlling not only human MC degranulation *in situ*, but also MC maturation from resident progenitors. Although there was a slight tendency to increased MC numbers and degranulation upon CB1 agonist stimulation (Fig. 3D-G), this was not significant. Furthermore, CB1 antagonist-induced hMMC degranulation was greatly reduced by CB1 agonists (Fig. 6A-C). This supports the general concept that “tonic” CB1 stimulation is primarily required to prevent *excessive* hMMC degranulation and maturation.[29]

Acknowledgements

The authors thank Claudia Kremling, Heike Krauth and Motoko Sugawara for excellent technical assistance. The generous professional support of Prof Masamitsu Ishii and Prof Hiromi Kobayashi, Osaka, for this work is also gratefully appreciated. Dr. Ewan Langan is gratefully acknowleged for editorial assistance. The NP organ culture approach taken here was inspired by Prof Gert Kunkel, Berlin[2].

REFERENCES

1. Moon TC, St Laurent CD, Morris KE, Marcet C, Yoshimura T, Sekar Y, et al. Advances in mast cell biology: new understanding of heterogeneity and function. Mucosal Immunol 2010;3:111-28. [PMID: 20043008]

2. Galli SJ, Tsai M. Mast cells in allergy and infection: versatile effector and regulatory cells in innate and adaptive immunity. Eur J Immunol 2010;40:1843-51. [PMID: 20583030]

3. Gibbs BF and Ennis M, Isolation and purification of human mast cells and basophils. Methods Mol Med 2001;56:161-176. [PMID: 21336900]

4. Howl J, Jones S and Farquhar M. Intracellular delivery of bioactive peptides to RBL-2H3 cells induces beta-hexosaminidase secretion and phospholipase D activation. ChemBioChem 2003;4:1312-1316. [PMID: 14661273]

5. Schierhorn K, Brunnée T, Paus R, Schultz KD, Niehus J, Agha-Mir-Salim P et al. Gelatin sponge-supported histoculture of human nasal mucosa. In Vitro Cell Dev Biol Anim 1995;31:215-20. [PMID: 7538857]

6. Patou J, Holtappels G, Affleck K, Gevaert P, Perez-Novo C, Van Cauwenberge P, et al. Enhanced release of IgE-dependent early phase mediators from nasal polyp tissue. J Inflamm (Lond) 2009;6:11. [PMID: 19379488]

7. Bentley AM, Hamid Q, Robinson DS, Schotman E, Meng Q, Assoufi B, et al. Prednisolone treatment in asthma. Reduction in the numbers of eosinophils, T cells, tryptase-only positive mast cells, and modulation of IL-4, IL-5, and interferon-gamma cytokine gene expression within the bronchial mucosa. Am J Respir Crit Care Med 1996;153:551-6 [PMID: 8564096]

8. Gilfillan AM, Austin SJ, Metcalfe DD. Mast cell biology: introduction and overview. Adv Exp Med Biol 2011;716:2-12. [PMID: 21713648]

9. Robinson DS. The role of the mast cell in asthma: induction of airway hyperresponsiveness by interaction with smooth muscle? J Allergy Clin Immunol 2004;114:58-65. [PMID: 15241345]

10. Okayama Y, Ra C, Saito H. Role of mast cells in airway remodeling. Curr Opin Immunol 2007;19:687-93. [PMID: 17761410]

11. Barnes PJ. Pathophysiology of allergic inflammation. Immunol Rev 2011;242:31-50. [PMID: 21682737]

12. Galli SJ, Tsai M, Piliponsky AM. The development of allergic inflammation. Nature 2008;454:445-54. [PMID: 18650915]

13. DeMarcantonio MA, Han JK. Nasal polyps: pathogenesis and treatment implications. Otolaryngol Clin North Am 2011;44:685-95. [PMID: 21621054]

14. Tan BK, Zirkle W, Chandra RK, Lin D, Conley DB, Peters AT, et al. Atopic profile of patients failing medical therapy for chronic rhinosinusitis. Int Forum Allergy Rhinol 2011;1:88-94. [PMID: 21731824]

15. Koh YI, Choi IS. Relationship between nasal and bronchial responsiveness in perennial allergic rhinitic patients with asthma. Int Arch Allergy Immunol 2002;129:341-7. [PMID: 12483039]

16. Hellings PW, Hessel EM, Van Den Oord JJ, Kasran A, Van Hecke P, Ceuppens JL. Eosinophilic rhinitis accompanies the development of lower airway inflammation and hyper-reactivity in sensitized mice exposed to aerosolized allergen. Clin Exp Allergy 2001;31:782-90. [PMID: 11422139]

17. Otsuka H, Inaba M, Fujikura T, Kunitomo M. Histochemical and functional characteristics of metachromatic cells in the nasal epithelium in allergic rhinitis: studies of nasal scrapings and their dispersed cells. J Allergy Clin Immunol 1995;96:528-36. [PMID: 7560665]

18. Elishmereni M, Alenius HT, Bradding P, Mizrahi S, Shikotra A, Minai-Fleminger Y et al. Physical interactions between mast cells and eosinophils: a novel mechanism enhancing eosinophil survival in vitro. Allergy 2011;66:376-85. [PMID: 20977491]

19. Verbruggen K, Van Cauwenberge P, Bachert C Anti-IgE for the treatment of allergic rhinitis--and eventually nasal polyps? Int Arch Allergy Immunol 2009;148:87-98. [PMID: 18799888]

20. Schierhorn K, Brunnée T, Schultz KD, Jahnke V, Kunkel G. Substance-P-induced histamine release from human nasal mucosa in vitro. Int Arch Allergy Immunol, 1995;107:109-114. [PMID: 7542055]

21. Bíró, T, Tóth IB, Haskó G, Paus R, Pacher P. The endocannabinoid system of the skin in health and disease: novel perspectives and therapeutic opportunities. Trends Pharmacol Sci 2009;30:411-20. [PubMed: 19608284]

22. Solinas M, Goldberg SR, Piomelli D. The endocannabinoid system in brain reward processes. Br J Pharmacol 2008;154:369-83. [PMID: 18414385]

23. Pertwee RG, Howlett AC, Abood ME, Alexander SP, Di Marzo V, Elphick MR et al., International Union of Basic and Clinical Pharmacology. LXXIX. Cannabinoid receptors and their ligands: beyond CB1 and CB2. Pharmacol Rev 2010;62:588-631. [PMID: 21079038]

501 24. Liu J, Wang L, Harvey-White J, Huang BX, Kim HY, Luquet S, et al. Multiple
502 pathways involved in the biosynthesis of anandamide. Neuropharmacology
503 2008;54:1-7. [PubMed: 17631919]

504 25. Di Marzo V, Piscitelli F, Mechoulam R. Cannabinoids and endocannabinoids in
505 metabolic disorders with focus on diabetes. Handb Exp Pharmacol 2011;(203):75-104.
506 [PMID: 21484568]

507 26. Cantarella G, Scollo M, Lempereur L, Saccani-Jotti G, Basile F, Bernardini R.
508 Endocannabinoids inhibit release of nerve growth factor by inflammation-activated
509 mast cells. Biochem Pharmacol 2011;82:380-8. [PMID: 21601562]

510 27. Cerrato S, Brazis P, della Valle MF, Miolo A, Puigdemont A. Effects of
511 palmitoylethanolamide on immunologically induced histamine, PGD2 and TNFalpha
512 release from canine skin mast cells. Vet Immunol Immunopathol 2010;133:9-15.
513 [PMID: 19625089]

514 28. De Filippis D, D'Amico A, Iuvone T. Cannabinomimetic control of mast cell
515 mediator release: new perspective in chronic inflammation. J Neuroendocrinol
516 2008;20 Suppl 1:20-5. [PMID: 18426495]

517 29. Sugawara K, Bíró T, Tsuruta D, Tóth IB, Kromminga A, Zákány N, et al.
518 Endocannabinoids limit excessive mast cell maturation and activation in human skin.
519 J Allergy Clin Immunol 2012;129:726-738 [PMID: 22226549]

520 30. Lu Z, Hasse S, Bodo E, Rose C, Funk W, Paus R. Towards the development of a
521 simplified long-term organ culture method for human scalp skin and its appendages
522 under serum-free conditions. Exp Dermatol 2007;16:37-44. [PMID: 17181635]

523 31. Ito N, Sugawara K, Bodó E, Takigawa M, van Beek N, Ito T, et al.
524 Corticotropin-releasing hormone stimulates the in situ generation of mast cells from
525 precursors in the human hair follicle mesenchyme. J Invest Dermatol
526 2010;130:995-1004. [PMID: 20043013]

527 32. Telek A, Bíró T, Bodó E, Tóth BI, Borbíró I, Kunos G, et al. Inhibition of human hair
528 follicle growth by endo- and exocannabinoids. FASEB J 2007;21:3534-3541.

529 33. Stone KD, Prussin C, Metcalfe DD. IgE, mast cells, basophils, and
530 eosinophils. J Allergy Clin Immunol 2010;125:S73-80. [PMID: 20176269]

531 34. Abramson J, Pecht I. Regulation of the mast cell response to the type 1 Fc epsilon
532 receptor. Immunol Rev 2007;217:231-54. [PMID:17498063]

533 35. Irani AA, Schechter NM, Craig SS, DeBlois G, Schwartz LB. Two types of human
534 mast cells that have distinct neutral protease compositions. Proc Natl Acad Sci U S A.
535 1986;83:4464-8. [PMID:3520574]

536 36. Okuda M. Functional heterogeneity of airway mast cells. Allergy. 1999;54 Suppl
537 57:50-62.

538 37. Dobrosi N, Tóth BI, Nagy G, Dózsa A, Géczy T, Nagy L, et al., Endocannabinoids
539 enhance lipid synthesis and apoptosis of human sebocytes via cannabinoid
540 receptor-2-mediated signaling. FASEB J. 2008;22:3685-95. [PMID: 18596221]

541 38. Galvao Nascimento N, Sampaio MC, Amaral Olivo R and Teixeira C. Contribution
542 of mast cells to the oedema induced by Bothrops moojeni snake venom and a
543 pharmacological assessment of the inflammatory mediators involved. Toxicon
544 2010;55:343-352. [PMID: 19703484]

545 39. Hennino A, Berard F, Guillot I, Saad N, Rozieres A and Nicolas JF. Pathology of
546 urticaria. Clin Rev Allergy Immunol 2006;30:3-11. [PMID: 16461989]

547 40. Braunstahl GJ, Overbeek SE, Fokkens WJ, Kleinjan A, McEuen AR, Walls AF, et
548 al. Segmental bronchoprovocation in allergic rhinitis patients affects mast cell and
549 basophil numbers in nasal and bronchial mucosa. Am J Respir Crit Care Med
550 2001;164:858-65. [PMID: 11549546]

551 41. Zhang G, Shao J, Su C, Zhao X, Wang X, Sun X et al., Distribution change of mast
552 cells in human nasal polyps. Anat Rec (Hoboken) 2012;295:758-63. [PMID:
553 22344830]

554 42. Takabayashi T, Kato A, Peters AT, Suh LA, Carter R, Norton J et al, Glandular
555 mast cells with distinct phenotype are highly elevated in chronic rhinosinusitis with
556 nasal polyps. J Allergy Clin Immunol 2012 [Epub ahead of print]. [PMID: 22534535]

557 43. Lamb JP, Sparrow MP. Three-dimensional mapping of sensory innervation with
558 substance p in porcine bronchial mucosa: comparison with human airways. Am J
559 Respir Crit Care Med 2002;166:1269-81. [PMID: 12403698]

560 44. Joos GF. The role of sensory neuropeptides in the pathogenesis of bronchial
561 asthma. Clin Exp Allergy 1989;19 Suppl 1:9-13. [PMID: 2653577]

562 45. Peters EM, Ericson ME, Hosoi J, Seiffert K, Hordinsky MK, Ansel JC, et al.
563 Neuropeptide control mechanisms in cutaneous biology: physiological and clinical
564 significance. J Invest Dermatol 2006;126:1937-47. [PMID: 16912691]

565 46. Arck P, Handjiski B, Hagen E, Pincus M, Bruenahl C, Bienenstock J, et al. Is there
566 a 'gut-brain-skin axis'? Exp Dermatol 2010;19:401-5. [PMID: 20113345]

567 47. Dinh QT, Suhling H, Fischer A, Braun A, Welte T. Innervation of the airways in
568 asthma bronchiale and chronic obstructive pulmonary disease (COPD). Pneumologie
569 2011;65:283-92. [PMID: 21271508]

570 48. Theoharides TC, Enakuaa S, Sismanopoulos N, Asadi S, Papadimas EC,
571 Angelidou A et al., Contribution of stress to asthma worsening through mast cell
572 activation. Ann Allergy Asthma Immunol 2012;109:14-19. [PMID: 22727152]

573 49. Otsuka H, Kusumi T, Kanai S, Koyama M, Kuno Y, Takizawa R. Stem cell factor
574 mRNA expression and production in human nasal epithelial cells: contribution to the
575 accumulation of mast cells in the nasal epithelium of allergy. J Allergy Clin Immunol
576 1998;102:757-64. [PMID: 9819292]

577 50. Liu C, Liu Z, Li Z and Wu Y. Molecular regulation of mast cell development and
578 maturation. Mol Biol Rep 2010;37:1993-2001. [PMID: 19644767]

579 51. Qi JC, Li L, Li Y, Moore K, Madigan MC, Katsoulotos G, Krilis SA. An antibody
580 raised against in vitro-derived human mast cells identifies mature mast cells and a
581 population of cells that are Fc epsilon RI(+), tryptase(-), and chymase(-) in a variety of
582 human tissues. J Histochem Cytochem 2003;51:643-53. [PMID: 12704212]

583 52. Ohnmacht C and Voehringer D. Basophil effector function and homeostasis during
584 helminth infection. Blood 2009;113:2816-2825. [PMID: 18941115]

585 53. Pawankar R. Nasal polyposis: an update: editorial review. Curr Opin in Allergy
586 Clin Immunology 2003;3:1-6. [PMID:12582307]

587 54. Jogie-Brahim S, Min HK, Fukuoka Y, Xia HZ and Schwartz LB. Expression of
588 alpha-tryptase and beta-tryptase by human basophils. J Allergy Clin Immunol
589 2004;113:1086-92. [PMID: 15208589]

590 55. Welker P, Grabbe J, Zuberbier T, Guhl S, Henz BM. Mast cell and myeloid marker
591 expression during early in vitro mast cell differentiation from human peripheral blood
592 mononuclear cells. J Invest Dermatol 2000;114(1):44-50 [PMID:10620114].

593

594

595 **Figure Legend** (60 words per each legend)

596

597 **FIG 1.** Human NP organ culture

598 PAS (**A**) and modified Verhoeff Van Gieson (**B**) histochemistry. Quantitative
599 immunohistomorphometry of (**C**) Ki67 in the epithelium and (**D**) lamina propria, (**E**)
600 TUNEL in lamina propria and (**F**) epithelium. BM=basement membrane, BV= blood
601 vessel, CF= collagen fibers. Data were obtained from 3 individuals. *****P<0.05, ******P<0.01,
602 *******P<0.001. N.S.=not significant.

603

604 **FIG 2.** hMMCs in organ cultured human NPs

605 (**A**) hMMCs histochemistry and immunohistochemistry. (**B**) Representative image of
606 degranulated tryptase+ hMMC. Quantitative tryptase (**C**)-, Kit (**D**)-
607 immunohistomorphometry. (**E**) SCF immunohistochemistry. Arrows: positive cells.
608 Arrow in (**E**): positive immunoreactivity. Data from 3 individuals. *****P<0.05, ******P<0.01.

609

610 **FIG 3.** hMMCs express functional CB1 *in situ*

611 (**A**) Kit/CB1 double immunofluorescence. Yellow arrow: double+ immunoreactivity. (**B**)
612 Kit (green) immunofluorescence with organ cultured NP treated with Tocrifluor (red).
613 Representative images of tryptase-immunohistochemistry (**C**). Yellow arrow:
614 non-degranulated hMMC. Red arrows: degranulated hMMCs. Quantitative
615 immunohistomorphometry of tryptase (**D** and **E**), %degranulation (**F** and **G**).

Data from 3 individuals. *****P<0.05, ******P<0.01, *******P<0.001. There was no significant difference between control and AEA/ACEA.

FIG 4. CB1 inhibition induces hMMC maturation but not proliferation

(**A**) Quantitative immunohistomorphometry of Kit. (**B**) %Ki67+ Kit+ cells in organ cultured human NPs. (**C**) %TUNEL+ Kit+ cells in organ cultured human NPs. (**D**) Quantitative immunohistomorphometry of chymase. (**E**) Representative images of tryptase+ hMMCs in the epithelium. (**F**) Quantitiative analysis of intraepithelial hMMCs. These experiments were from 3 individuals. ******P<0.01, *******P<0.001, N.S.=not significant.

FIG 5. CB1 blockade by gene knock-down increases hMMC number and induces degranulation *in situ*

(**A**) CB1 immunohistochemistry. TFE=transfection reagent-, SCR=scrambled siRNA-, CB1 siRNA=CB1 siRNA- treated NPs. Quantitative analysis of relative CB1 immunoreactivity within the epithelium (**B**) and CB1+ mesenchymal cells (**C**). Percentages of tryptase+ (**D**) and degranulated (**E**) hMMCs among TFE, SCR or CB1 siRNA treated NPs. These experiments were from 2 individuals. *****P<0.05, ******P<0.01, *******P<0.001.

FIG 6. CB1 stimulation inhibits hMMCs degranulation by MC secretagogues

Percentage of degranulated tryptase+ hMMCs in organ cultured human NPs after stimulation with MC secretagogues, substance P (**A**, 10^{-10}M), compound 48/80 (**B**, 10 μg/ml) and CRH (**C**, 10^{-7}M) in combination with AEA (30 μM) or ACEA (30 μM). AEA or ACEA clearly inhibited hMMC degranulation by various MC secretagogues. *****P<0.05, **P<0.01, *******P<0.001. These experiments were from 2 individuals.

FIG 7. CB1 inhibition increases SCF expression *in situ*

(**A**) Representative images of SCF immunofluorescence in NP epithelium. Arrow denotes SCF+ immunoreactivity. (**B**) Quantitative SCF immunohistomorphometry. (**C**) %tryptase+ hMMC in organ cultured human NPs (1 day). AEA, ACEA: 30 μM, AM251: 1 μM, anti-SCF neutralizing antibody: 1 μg/ml. These experiments were from 2 individuals. *****P<0.05, *******P<0.001.

650

651 Cannabinoid receptor-1 controls human 652 mucosal-type mast cell degranulation and 653 maturation *in situ*

654

655 Koji Sugawara[1,2], Nóra Zákány[1,3*], Torsten Hundt[1*], Vladimir Emelianov[1#], Daisuke
656 Tsuruta[2], Christian Schäfer[4], Jennifer E. Kloepper[1], Tamás Bíró[3] and Ralf Paus[1,5]

657

658

659

660

661 **Supplementary Information**

662

663 **Contents:**

668

Supplementary Material and Methods

Reagents

N-arachidonoylethanolamine (AEA), arachidonyl-2-chloroethylamide (ACEA), N-(piperidin-1-yl)-1-(2,4-dichlorophenyl)-5-(4-chlorophenyl)-4-methyl-1H-pyrazole-3-carboxamide (AM251), substance P, compound 48/80 and corticotropin-releasing hormone (CRH) were purchased from Sigma-Aldrich (Taufkirchen, Germany), whereas 5-carboxytetramethylrhodamine (5-TAMRA) conjugated AM251, Tocrifluor was from Tocris Bioscience (Bristol, UK). SCF- neutralizing antibody was from R&D systems (R&D systems, Minneapolis, MN). The sources of the primary antibodies used for immunohistochemistry/immunofluorescence are indicated below.

Histochemistry

Histochemistry for collagen fibers was performed according to manufacture's protocol (modified Verhoeff Van Gieson stain, Elastic stain Kit, Sigma). For PAS staining, deparaffinized sections were incubated with 1% periodic acid at RT (room temperature) for 10 min. After a wash, the sections were incubated with Schiff's reagent (Merck, Darmstadt, Germany) at RT for 15 min, followed by a wash with tap water. Then, the sections were counterstained by Hematoxylin. Leder's esterase histochemistry was performed with cryo-embeded sections as previously reported.[E1]

We define a mast cell (MC) as "degranulated", when 5 or more histochemically or immunohistologically identified MC granules are seen to be located clearly outside the

cell membrane. Although a cut-off set at 5 extracellular MC granules is evidently arbitrary and likely only captures MCs that are undergoing “anaphylactic” MC degranulation,[E2] this simple, but pragmatic and easily reproducible morphometric technique has proven very instructive and sensitive in multiple previous MC *in situ* studies that we and others have published in murine and human skin.

Immunohistochemistry/Immunofluorescence microscopy

For the detection of Kit, tryptase and chymase, deparaffinized sections were antigen-retrieved by microwave (650 W, 20 minutes [min]). After the pre-incubation with either 5% normal goat serum + 1% BSA in 0.05 M Tris–HCl buffered saline (TBS) (RT, 60 min, for Kit) or 0.5% triton-X in 6% BSA in TBS (RT, 30 min, for chymase, tryptase and FcεRIα), sections were incubated overnight at 4°C with primary antibodies, rabbit anti-human CD117 (DAKO, Hamburg, Germany) at 1:100, mouse anti-human chymase (Abcam plc, Cambridge, UK) at 1:100, mouse anti-FcεRIα (Acris Antibodies GmbH, Herford, Germany) at 1:100, or mouse anti-human tryptase (Abcam plc) at 1:500 diluted in antibody diluent (DCS Innovative Diagnostik-Systeme, Hamburg, Germany). Thereafter, the sections were incubated with goat biotinylated antibodies against rabbit or mouse IgG (Jackson Immunoresearch Laboratories, West Grove, PA) at 1:200 in antibody diluents (DCS Innovative Diagnostik-Systeme) for 45 min at RT. Sections were then treated with the alkaline phosphatase-based avidin-biotin complex (Vectastain Elite ABC kit; Vector Laboratories, Burlingame, CA) and the expression of these antigens was visualized by Fast Red (Sigma).

For the detection of cannabinoid receptor 1 (CB1), after deparaffinization and antigen-retrieval, the sections were pretreated with avidin and biotin (Blocking Kit, Vector Laboratories) to block the endogenous avidin and biotin. After the overnight incubation with the primary anti-CB1 antibody (Santa Cruz, 1:50 in antibody diluents), the sections were treated by alkaline phosphatase-based labeled streptoavidin biotin method (DCS Innovative Diagnostik-Systeme) and CB1 expression was visualized by Fast Red (Sigma).

Double-immunostaining for Kit and CB1 was performed by using the tyramide signal amplification (TSA) technique (Perkin Elmer, Boston, MA).[E1]

For double-immunohistochemistry for Kit and FcεRIα, the sections were first deparaffinized and antigen-retrieved by microwave. After the overnight incubation with mouse anti-FcεRIα at 1:100 (at 4°C), slides were incubated with biotin conjugated goat anti-mouse IgG at 1:200 for 45 min (at RT). Sections were then treated by HRP-based avidin-biotin complex (Vectastain Elite ABC kit; Vector Laboratories) and FcεRIα expression was visualized by DAB (Dako). After the careful wash, the sections were then overnight-incubated with rabbit anti-CD117 antibody at 1:100 (at 4°C). Thereafter, the sections were incubated with goat biotinylated antibodies against rabbit IgG (Jackson Immunoresearch Laboratories) at 1:200 for 45 min at RT. Sections were then treated with the alkaline phosphatase-based avidin-biotin complex (Vectastain Elite ABC kit; Vector Laboratories) and the expression of these antigens was visualized by Fast Red (Sigma).

To study the proliferation or apoptosis of the Kit+ cells, double-immunostaining for Ki67 and Kit or Kit immunostaining and terminal dUTP nick-end labeling (TUNEL) was performed on the same cryo-embeded sections as we have previously shown.[E1]

For detecting SCF in cryo-embeded organ cultured human NPs, an indirect immunofluorescence method was applied,[E1] while alkaline phosphatase-based avidin-biotin method was performed on paraffin-embedded sections using rabbit anti-human SCF antibody at 1:50 (Santa Cruz) and the expression of the antigen was visualized by Fast Red (Sigma).

For detecting double+ cells for tryptase and chymase within human NPs, the double-immunostaining could not be successfully performed since the primary antibodies for tryptase and chymase were from same species. Therefore, we performed these immunostaining separately using a pair of "mirror image" sections, so that we could take advantage of the possible detection of two different staining patterns in exactly the same cell within the tissue.[E3]

Quantitative immunohistomorphometry

Antigen expression was quantified by assessing the immunoreactivity in defined reference areas was assessed by quantitative immunohistomorphometry[E1] using the ImageJ software (National Institutes of Health, Bethesda, MD).

High resolution light microscopy (HRLM) and Transmission electron microscopy (TEM)

762 Thin and thick sections of organ cultured human NPs were generated as previously
763 reported.[E1] 1 μm of thick sections were prepared for an alkaline Giemsa
764 histochemistry,[E1] while thin sections were stained with uranyl acetate and lead citrate
765 and observed with an electron microscope (JEM-1200EXII, JEOL, Tokyo, Japan).[E1]

766

767 **LDH measurement**

768 Lactate dehydrogenase (LDH) activity in the culture medium was measured according
769 to the manufacturer's instructions (Cytotoxicity Detection Kit, Roche Mannheim,
770 Germany) as a biochemical indicator of tissue viability.[E4] The absorbance of the
771 samples was measured at 490 nm using an ELISA reader.

772

773 **CB1 knock-down *in situ***

774 All reagents required for transfection (human CB1 siRNA (sc-39910), control
775 (scrambled, SCR) siRNA (sc-37007), siRNA transfection reagent (sc-29528) and
776 siRNA transfection Medium (sc-36868)) were obtained from Santa Cruz. Transfection
777 (6 hrs) with isolated human NPs was performed as described previously.[E1]

778

779

780

Supplementary texts

S1. Giannini et al[E5] reported that a non-selective CB1/CB2 agonist (CP55,940) prevented antigen-induced asthma-like reaction in guinea pigs and that this effect was abrogated by the treatment with either CB1 or CB2 antagonists. Interestingly, the degranulation-protective effect of CP55,940 on guinea pig lung MCs was abrogated by co-administration of the CB1 specific antagonist, AM251, but not by a CB2-specific antagonist. Yet, the authors concluded that both receptors might be important to inhibit guinea pig lung MC degranulation.[E5]

S2. While MCs represent by far the largest c-Kit+ cell population in human and murine skin mesenchyme, it was unclear whether this also applies to human NPs. However, FcεRIα and Kit double-immunohistochemistry (Fig. E1D) revealed that, 71.3% of Kit+ cells co-expressed FcεRIα in freshly microdissected human NP samples (n=3). Therefore, most Kit+ cells in human NP stroma clearly represent hMMCs. hMMCs have been reported to express tryptase, but not chymase.[E6,7] However, human tissues display mixed MC sub-types, and MC distribution, which are not as clearly demarcated as in rodents.[E8] Indeed, in freshly isolated human NP samples, the ratio of MCT (tryptase+, chymase- MCs; which likely represent T-cell dependent mucosal MCs[E9]) versus MCTC (tryptase+, chymase+) was 76.87% : 23.13% in epithelium, while that in lamina propria was 66.85% : 33.15% detected by tryptase or chymase immunohistochemistry using “Mirror image” sections (see supplementary Methods) (from 2 individuals) (Fig. E1E).

References

E1. Sugawara K, Bíró T, Tsuruta D, Tóth IB, Kromminga A, Zákány N, et al. Endocannabinoids limit excessive mast cell maturation and activation in human skin. J Allergy Clin Immunol 2012;129:726-738.e8. [PMID: 22226549]

E2. Dvorak AM, Massey W, Warner J, Kissell S, Kagey-Sobotka A, Lichtenstein LM Blood 1991;77:569-78. [PMID 1703796]

E3. Sugawara K, Tsuruta D, Kobayashi H, Ikeda K, Hopkinson SB, Jones JC et al., J Histochem Cytochem 2007;55:43-55. [PMID: 16957169]

E4. Lu Z, Hasse S, Bodo E, Rose C, Funk W, Paus R. Towards the development of a simplified long-term organ culture method for human scalp skin and its appendages under serum-free conditions. Exp Dermatol 2007;16:37-44. [PMID: 17181635]

E5. Giannini L, Nistri S, Mastroianni R, Cinci L, Vannacci A, Mariottini C, et al. Activation of cannabinoid receptors prevents antigen-induced asthma-like reaction in guinea pigs. J Cell Mol Med 2008;12:2381-94. [PMID: 18266975]

E6. Irani AA, Schechter NM, Craig SS, DeBlois G, Schwartz LB. Two types of human mast cells that have distinct neutral protease compositions. Proc Natl Acad Sci U S A. 1986;83:4464-8. [PMID:3520574]

E7. Okuda M. Functional heterogeneity of airway mast cells. Allergy. 1999;54 Suppl 57:50-62. [PMID: 10565486]

E8. Moon TC, St Laurent CD, Morris KE, Marcet C, Yoshimura T, Sekar Y, et al. Advances in mast cell biology: new understanding of heterogeneity and function. Mucosal Immunol 2010;3:111-28. [PMID: 20043008]

827 E9. Xing W, Austen KF, Gurish MF and Jones TG. Protease phenotype of connective
828 tissue and of induced mucosal mast cells in mice is regulated by the tissue. Proc Natl
829 Acad Sci U S A. 2011;108:14210-5 [PMID: 21825171]

830

831

832

833

834

Supplementary Figure legend

FIG E1. hMMCs are detectable by MC immunohistochemistry during the organ culture

(**A**) tryptase+degranulated MC. yellow allows: MC granules outside cell membrane. (**B**) LDH assay. (**C**) hMMCs (alkaline Giemsa histochemistry) (**D**) Kit/FcεRIα immunohistochemistry. Black arrows: FcεRIα+ cells. Red arrow: Kit+ cells. Yellow arrow: double+ cell. (**E**) tryptase/chymase "mirror image"-immunohistochemistry. Red arrow: tryptase+ chymase- cells. Yellow arrows: double+ cells. Quantitative tryptase (**F**), Kit (**G**) immunohistomorphometry. From 3 individuals. *P<0.05, **P<0.01, ***P<0.001, N.S.=not significant.

FIG E2. CB1 inhibition promotes the degranulation of hMMCs in NPs.

(**A**) Quantitative Ki67/Kit immunohistomorphometry. (**B** and **C**) Quantitative tryptase immnuohistomorphometry (**D**) Quantitative alkaline Giemsa histomorphometry of hMMCs. (**E**) Transmission electron microscopy of hMMCs. Yellow arrow: Non-degranulated hMMC. Red arrow: Degranulated hMMC. Quantitative Kit (**G**) and chymase (**H**) immunohistomorphometry Data were from 2-3 individuals. *P<0.05, **P<0.01, ***P<0.001, N.S.=not significant.

FIG E3. CB1 inhibition increased the percentage of tryptase+ hMMCs in all samples examined

Tryptase immunohistomorphometry. *P<0.05, **P<0.01.

FIG E4. CB1 inhibition induced tryptase+ hMMCs degranulation in all samples examined

Tryptase immunohistomorphometry. ***P<0.05, ****P<0.01, *****P<0.001.

FIG E5. CB1 inhibition increased the percentages of Kit+ and chymase+ hMMCs in all samples examined

Left side: Quantitative Kit immunohistomorphometry of organ cultured human NP samples treated with either vehicle or AM251 (1 μM).

Right side: Quantitative chymase immunohistomorphometry of organ cultured human NP samples treated with either vehicle or AM251 (1 μM). ***P<0.05, ****P<0.01.

FIG E6. CB1 inhibition induced edema in lamina propria within organ cultured human NPs

(**A**) Representative images on cellularity (by tryptase immunohistochemistry) of organ cultured human NPs treated with either vehicle (control) or AM251. Red arrows indicate tryptase+ cells. Quantitative analysis of cellularity in lamina propria (**B**). *****P<0.001. These experiments were from 2-3 individuals.

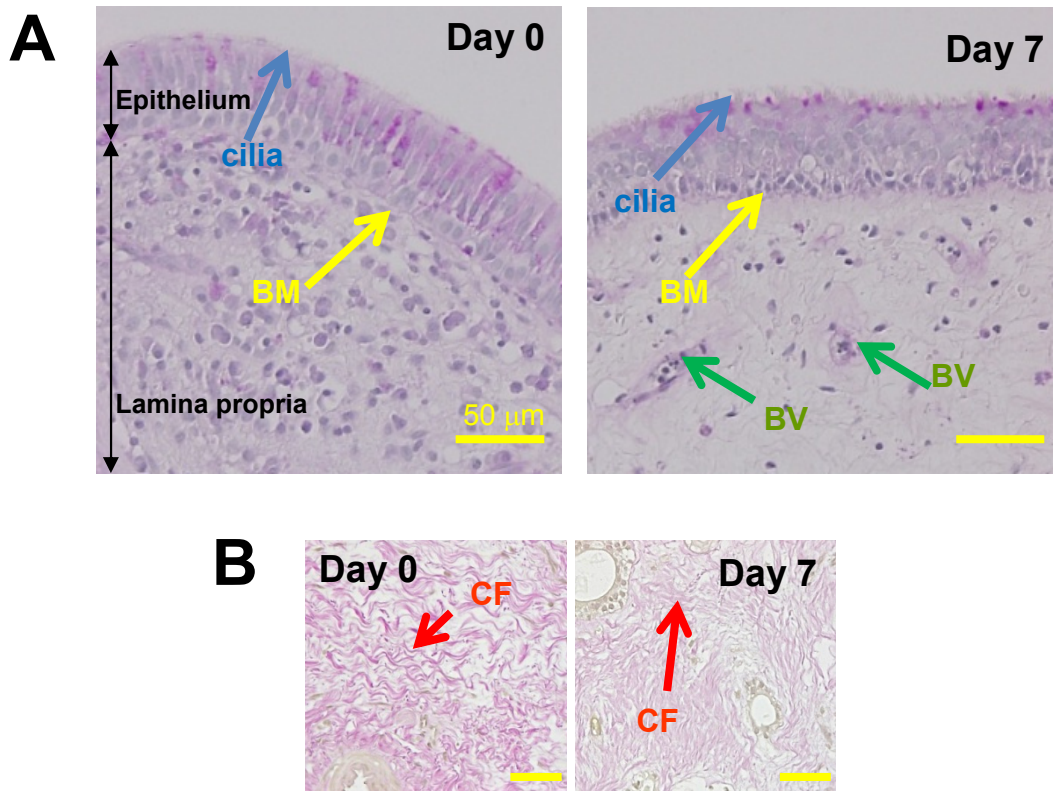
A
Day 0
Epithelium
cilia
BM
Lamina propria
50 μm
Day 7
cilia
BM
BV
BV
B
Day 0
CF
Day 7
CF

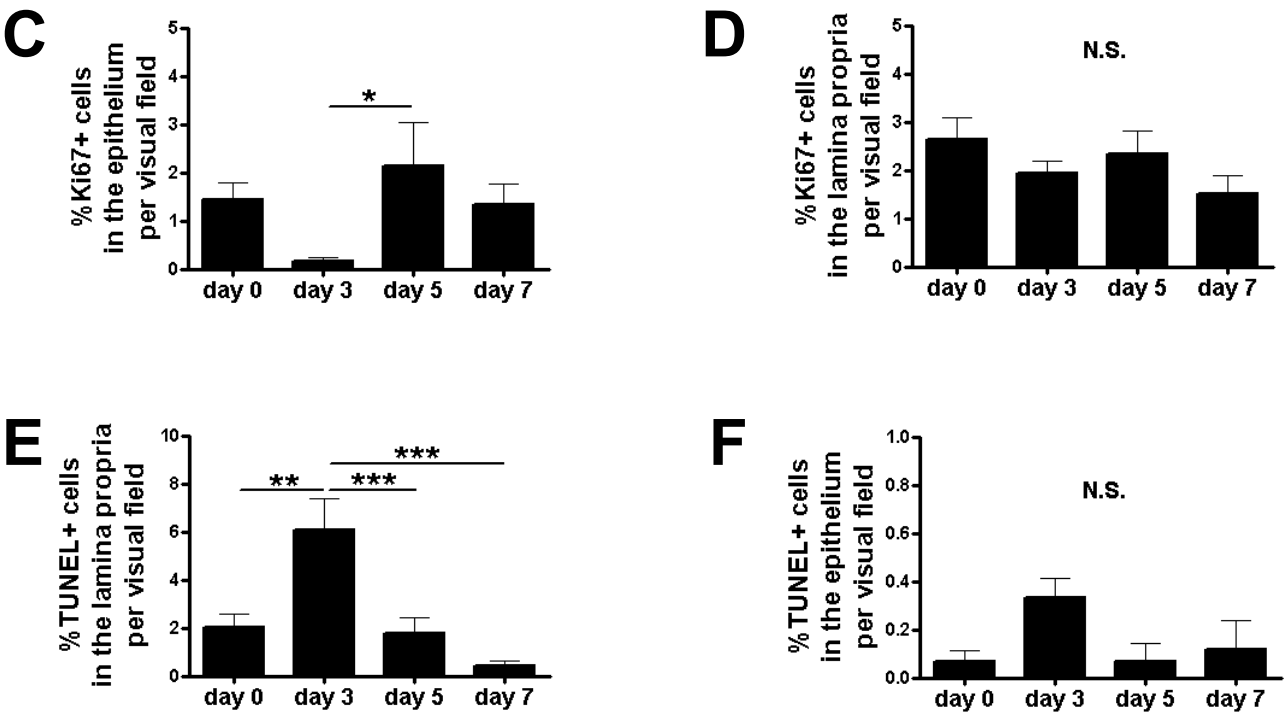
C
% Ki67+ cells in the epithelium per visual field
*
day 0
day 3
day 5
day 7
D
% Ki67+ cells in the lamina propria per visual field
N.S.
day 0
day 3
day 5
day 7
E
% TUNEL+ cells in the lamina propria per visual field
**
***
***
day 0
day 3
day 5
day 7
F
% TUNEL+ cells in the epithelium per visual field
N.S.
day 0
day 3
day 5
day 7

FIG 1.

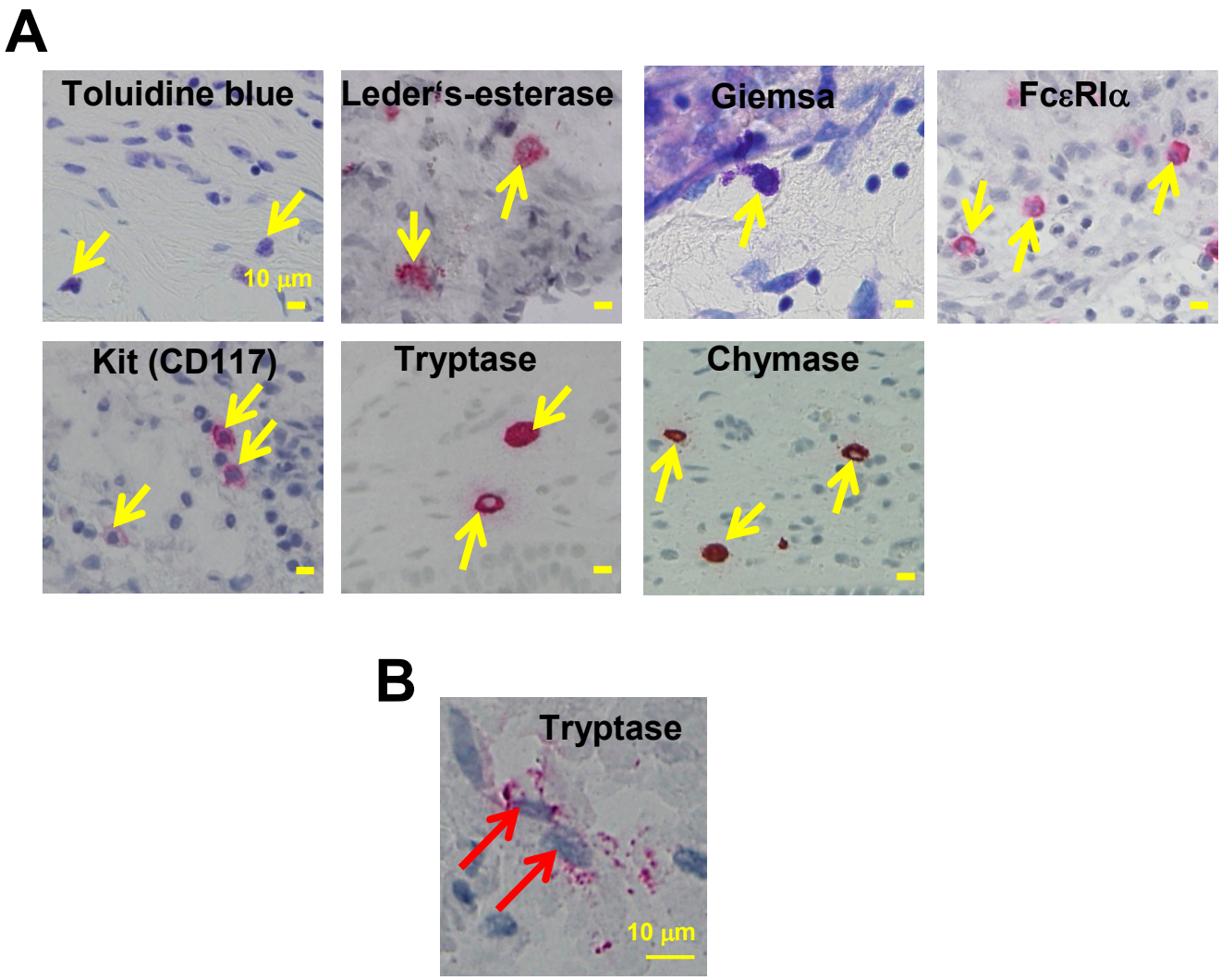
A
Toluidine blue
10 μm
Leder's-esterase
Giemsa
FcεRIα
Kit (CD117)
Tryptase
Chymase
B
Tryptase
10 μm
C
%tryptase+ MCs/total nuclei per visual field
15
10
5
0
**
day 0
day 3
day 5
day 7
D
%Kit+ MCs/total nuclei per visual field
6
4
2
0
*
day 0
day 3
day 5
day 7
E
SCF
Day 7
10 μm
negative

FIG 2.

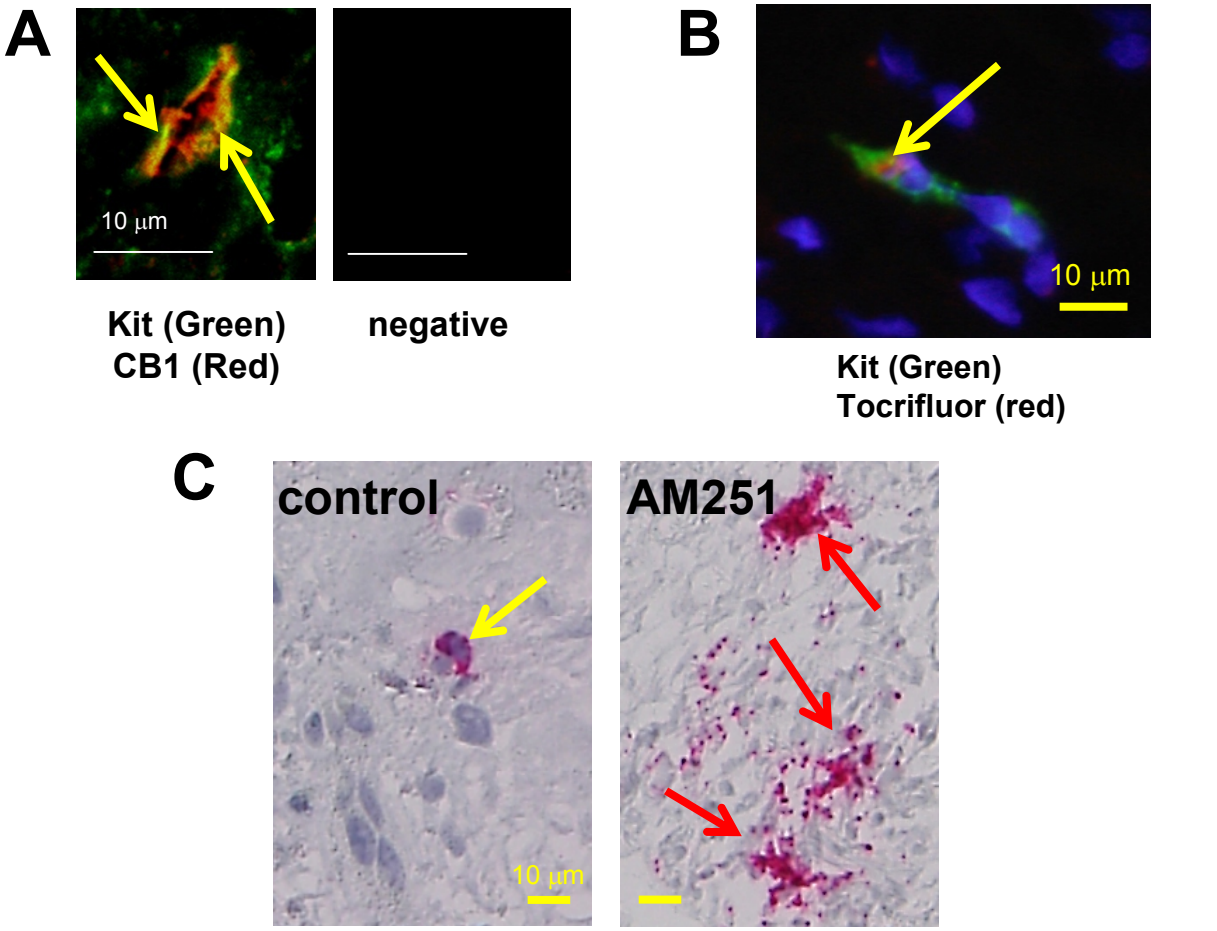
A
10 μm
Kit (Green)
CB1 (Red)
negative
B
10 μm
Kit (Green)
Tocrifluor (red)
C
control
AM251
10 μm
D
%tryptase+ MCs/total nuclei per visual field
2.5
2.0
1.5
1.0
0.5
0.0
**
**
control
ACEA
AM251
ACEA+AM251
E
%tryptase+ MCs/total nuclei per visual field
3
2
1
0
***
control
AEA
AM251
AEA+AM251
F
%degranulation per visual field
15
10
5
0
***
***
***
control
ACEA
AM251
ACEA+AM251
G
%degranulation per visual field
25
20
15
10
5
0
***
***
*
control
AEA
AM251
AEA+AM251

FIG 3.

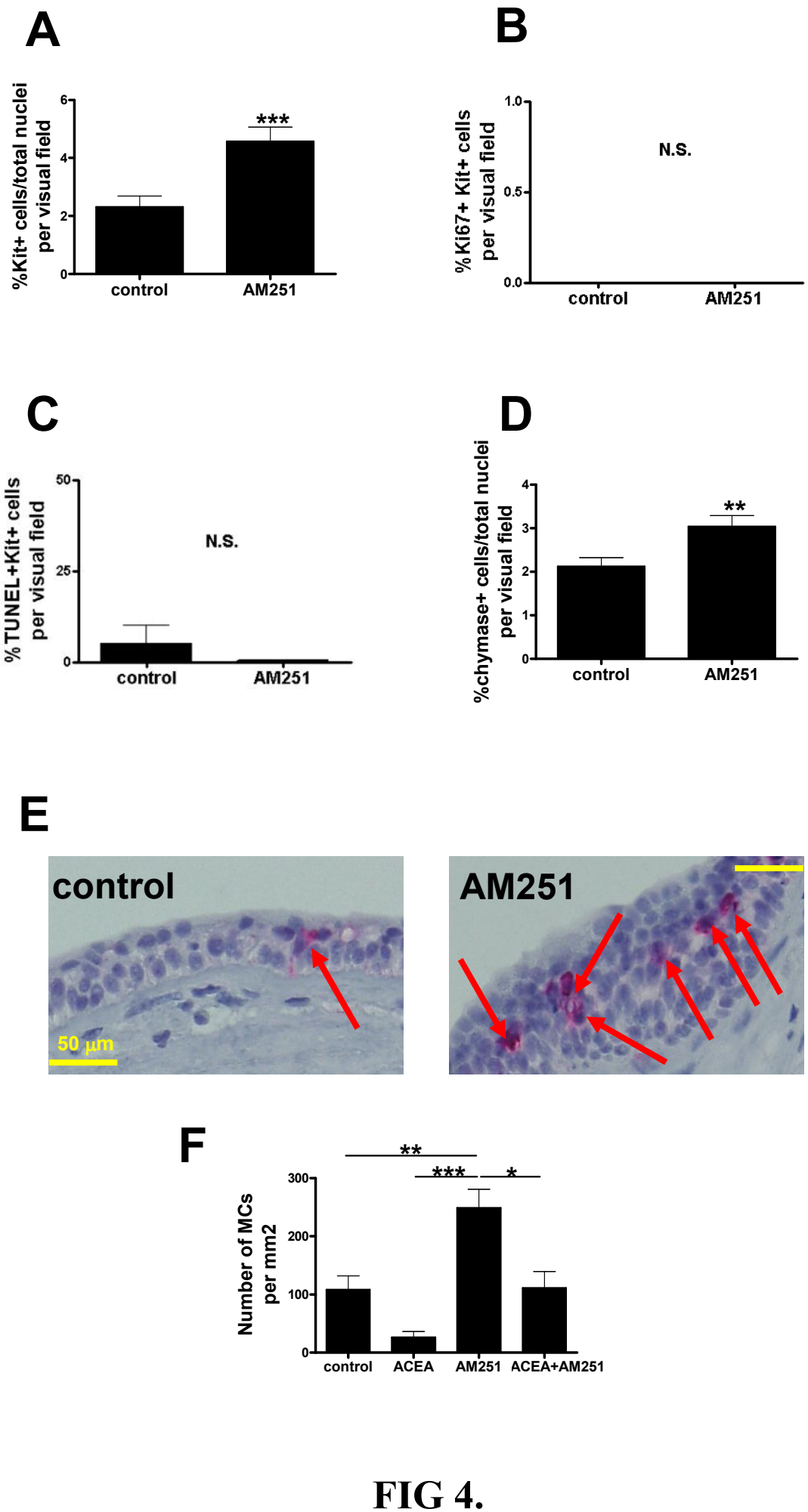
A
%Kit+ cells/total nuclei per visual field
6
4
2
0
***
control
AM251
B
% Ki67+ Kit+ cells per visual field
1.0
0.5
0.0
N.S.
control
AM251
C
% TUNEL+Kit+ cells per visual field
50
25
0
N.S.
control
AM251
D
%chymase+ cells/total nuclei per visual field
4
3
2
1
0
**
control
AM251
E
control
50 µm
AM251
F
Number of MCs per mm2
300
200
100
0
**
***
*
control
ACEA
AM251
ACEA+AM251

FIG 4.

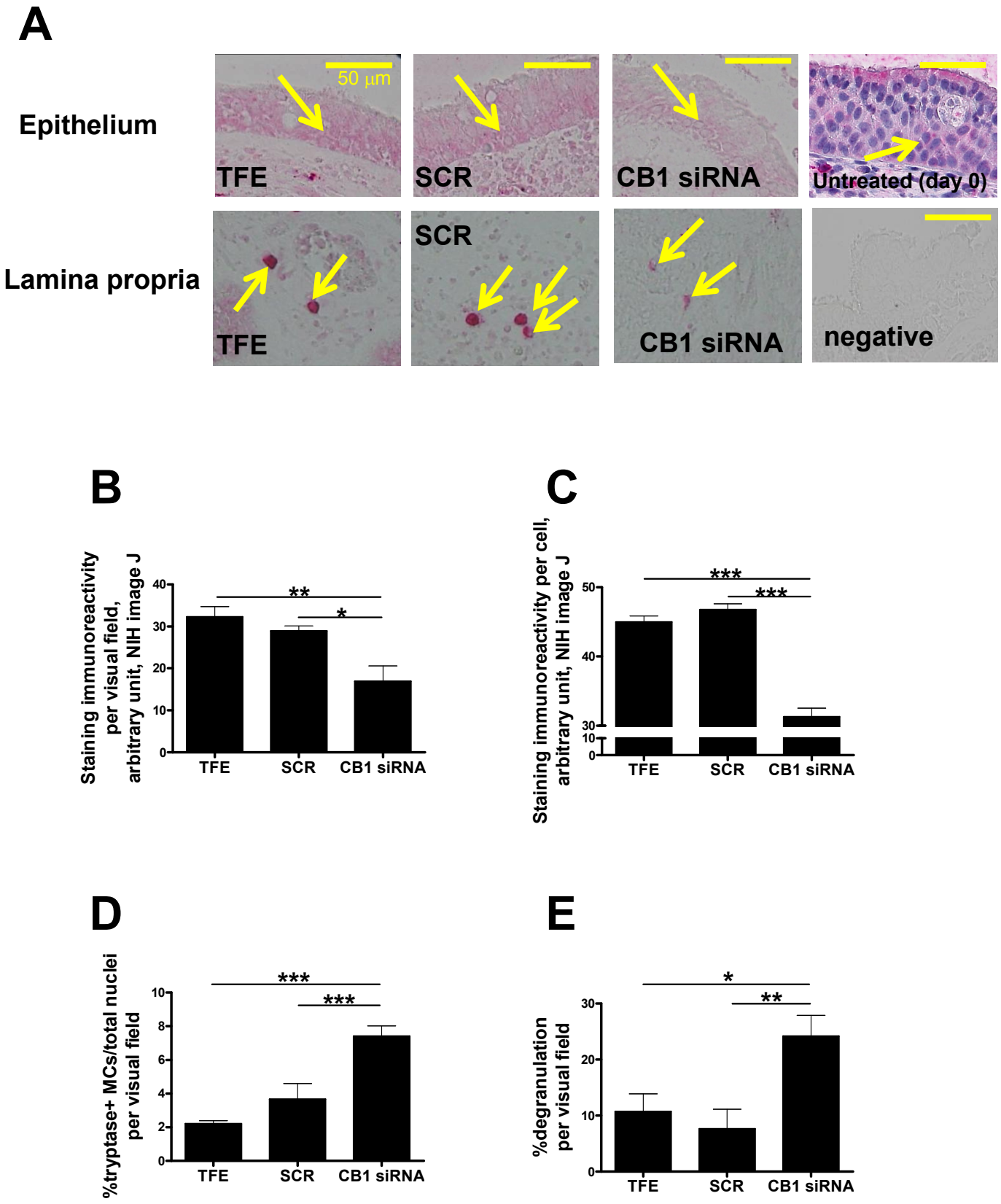
A
Epithelium
Lamina propria
50 µm
TFE
SCR
CB1 siRNA
Untreated (day 0)
TFE
SCR
CB1 siRNA
negative
B
Staining immunoreactivity per visual field, arbitrary unit, NIH image J
**
*
TFE
SCR
CB1 siRNA
C
Staining immunoreactivity per cell, arbitrary unit, NIH image J
***
***
TFE
SCR
CB1 siRNA
D
%tryptase+ MCs/total nuclei per visual field
***
***
TFE
SCR
CB1 siRNA
E
%degranulation per visual field
*
**
TFE
SCR
CB1 siRNA

FIG 5.

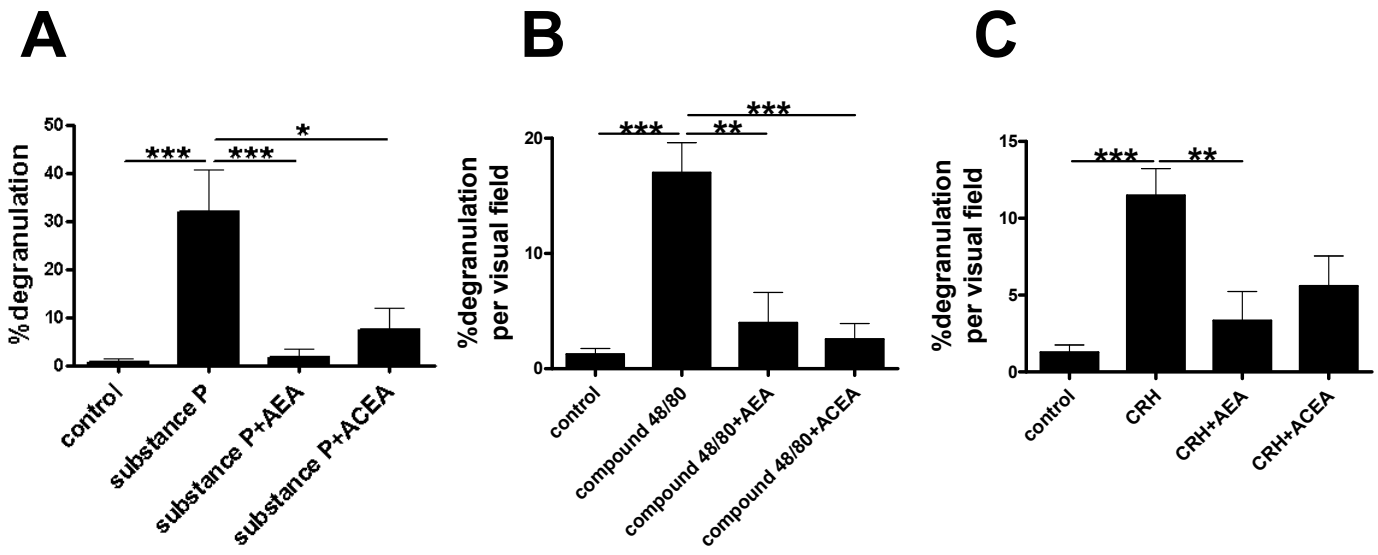
A
%degranulation
50
40
30
20
10
0
***
***
*
control
substance P
substance P+AEA
substance P+ACEA
B
%degranulation per visual field
20
10
0
***
**
***
control
compound 48/80
compound 48/80+AEA
compound 48/80+ACEA
C
%degranulation per visual field
15
10
5
0
***
**
control
CRH
CRH+AEA
CRH+ACEA

FIG 6.

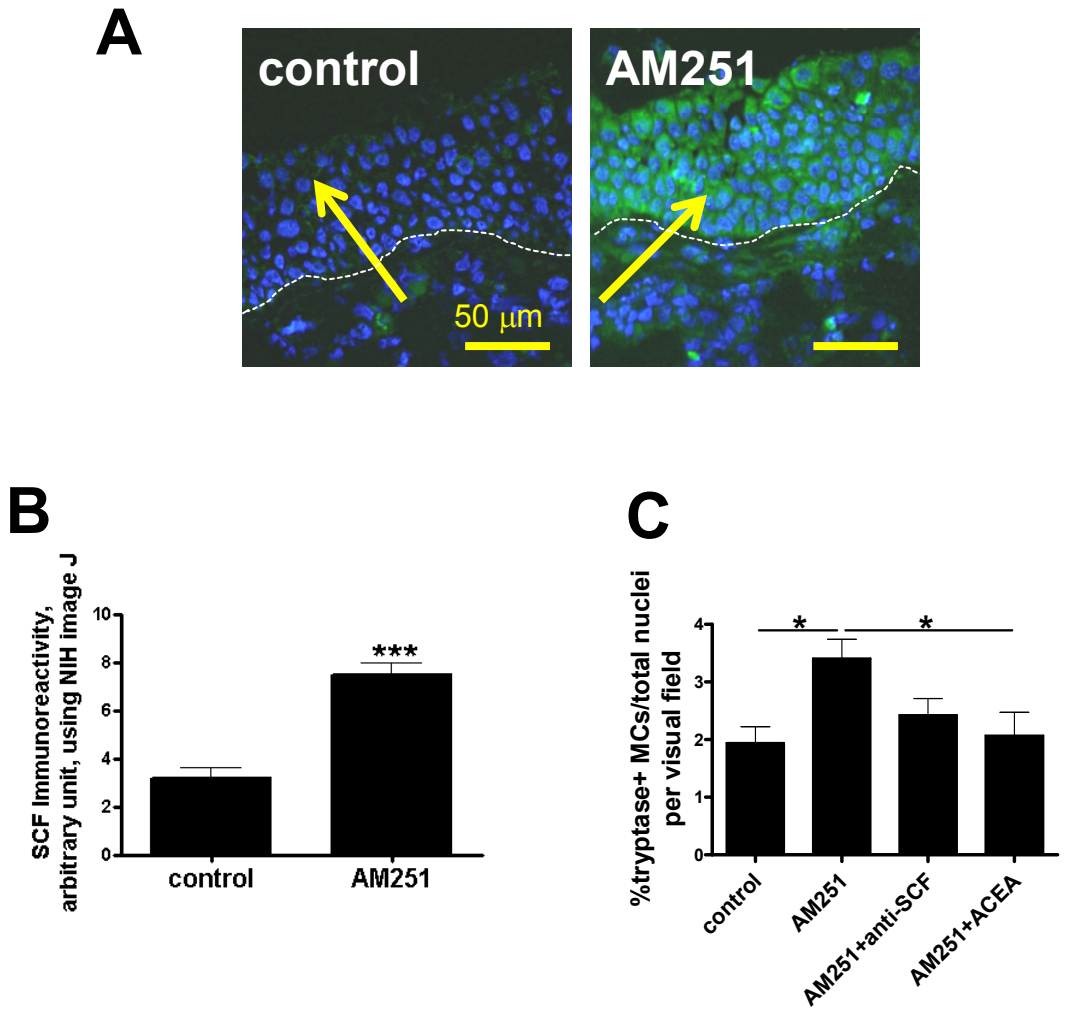
A
control
AM251
50 μm
B
SCF Immunoreactivity, arbitrary unit, using NIH image J
10
8
6
4
2
0
***
control
AM251
C
%tryptase+ MCs/total nuclei per visual field
4
3
2
1
0
*
*
control
AM251
AM251+anti-SCF
AM251+ACEA

FIG 7.

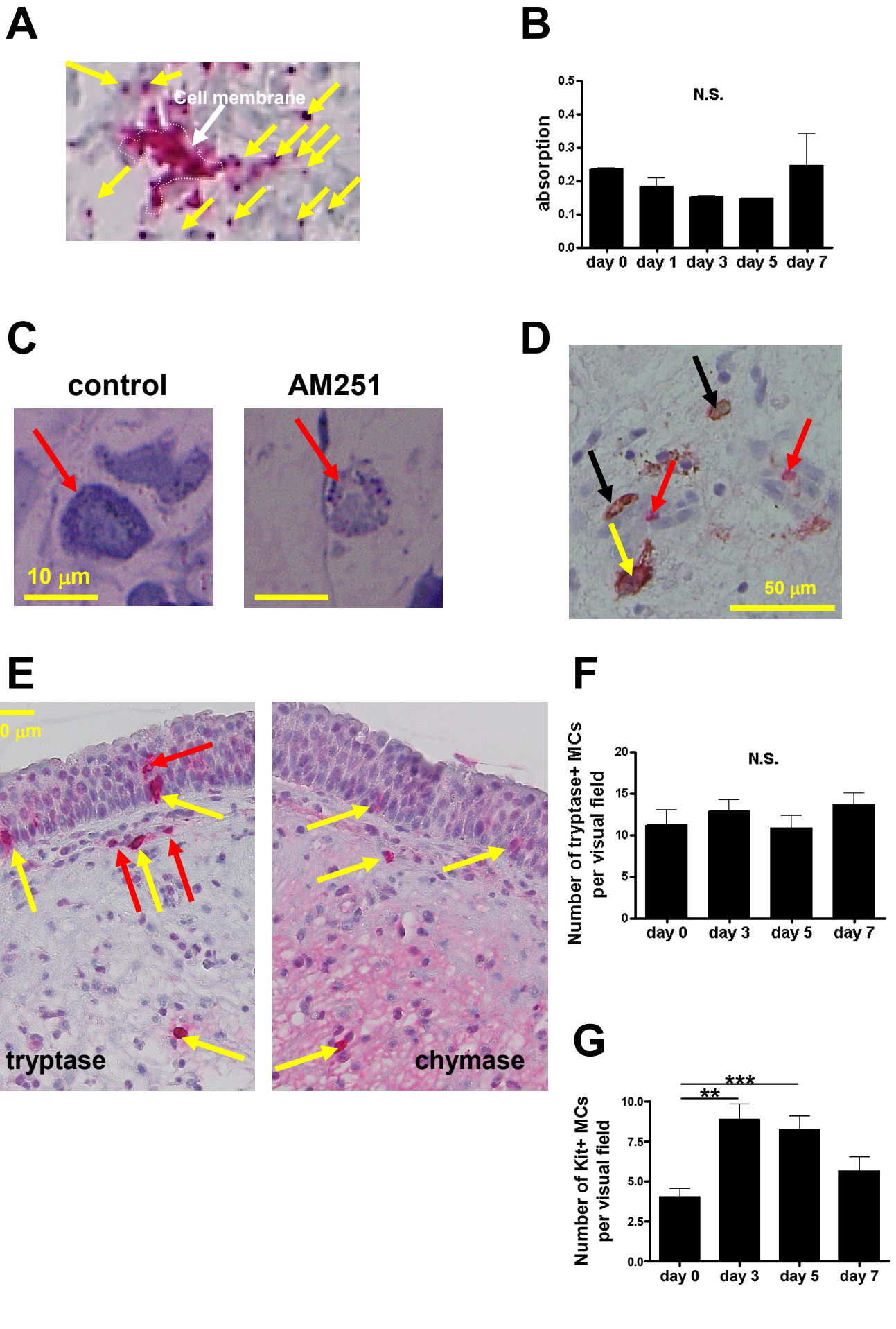
A
Cell membrane
B
N.S.
absorption
0.5
0.4
0.3
0.2
0.1
0.0
day 0
day 1
day 3
day 5
day 7
C
control
AM251
10 μm
D
50 μm
E
50 μm
tryptase
chymase
F
N.S.
Number of tryptase+ MCs per visual field
20
15
10
5
0
day 0
day 3
day 5
day 7
G
***
**
Number of Kit+ MCs per visual field
10.0
7.5
5.0
2.5
0.0
day 0
day 3
day 5
day 7

FIG E1.

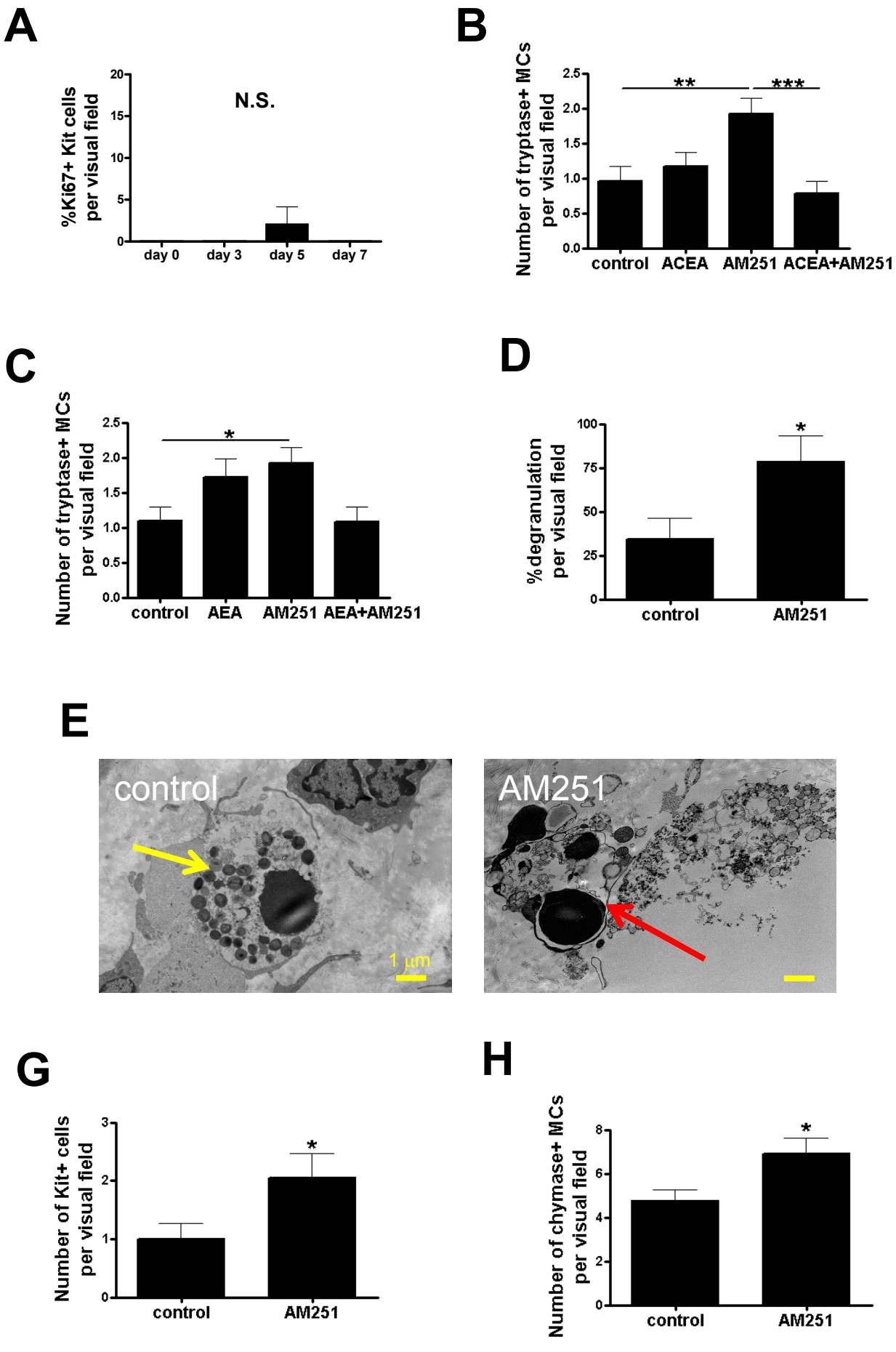
A
%Ki67+ Kit cells per visual field
N.S.
day 0
day 3
day 5
day 7
B
Number of tryptase+ MCs per visual field
**
***
control
ACEA
AM251
ACEA+AM251
C
Number of tryptase+ MCs per visual field
*
control
AEA
AM251
AEA+AM251
D
%degranulation per visual field
*
control
AM251
E
control
1 µm
AM251
G
Number of Kit+ cells per visual field
*
control
AM251
H
Number of chymase+ MCs per visual field
*
control
AM251

FIG E2.

Patient 1.

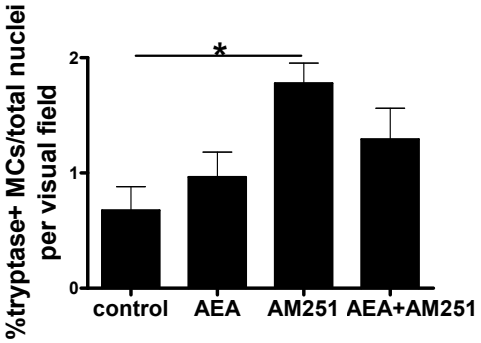

Patient 1.

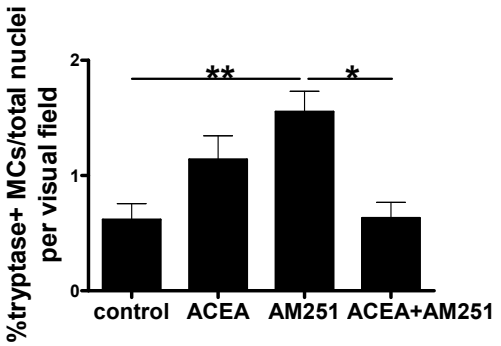

Patient 2.

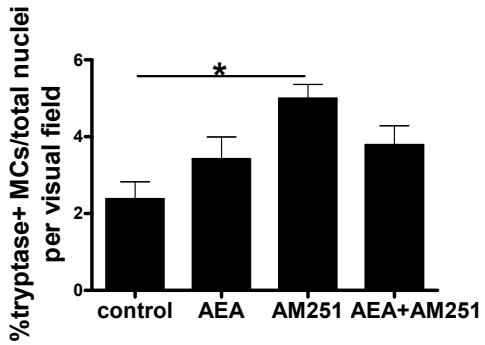

Patient 3.

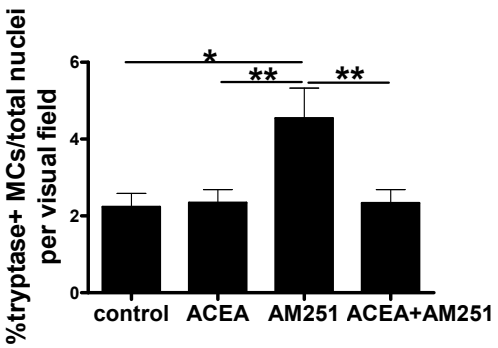

Patient 4.

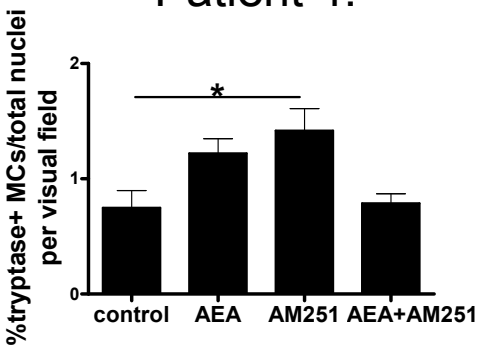

Patient 4.

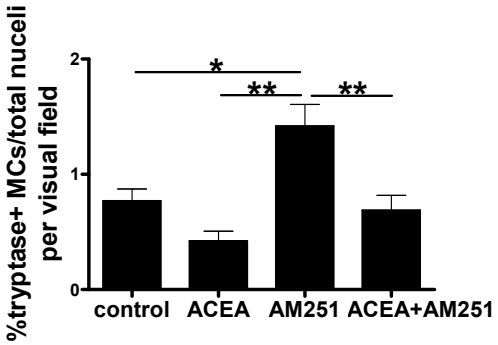

FIG E3.

Patient 1.

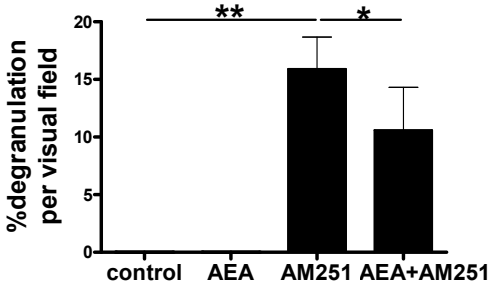

Patient 1.

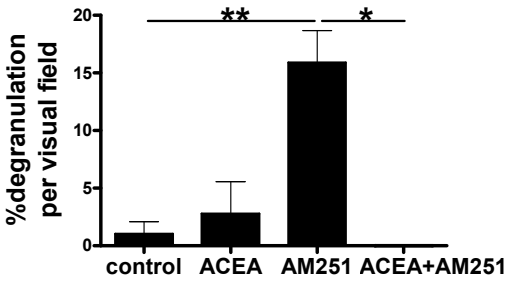

Patient 2.

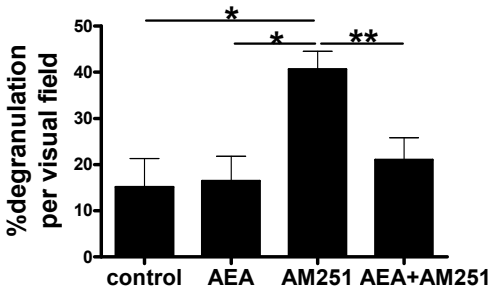

Patient 3.

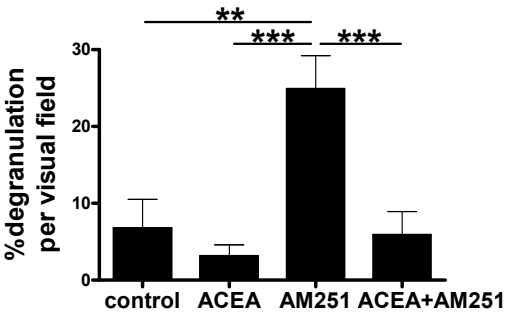

Patient 4.

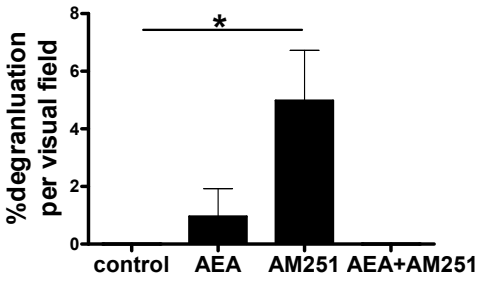

Patient 4.

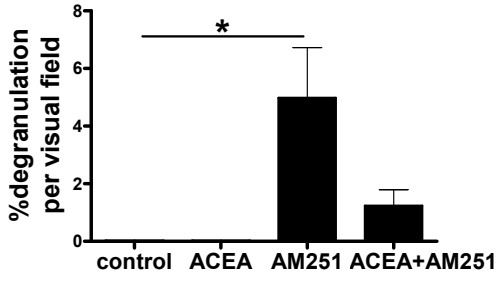

FIG E4.

Patient 1.

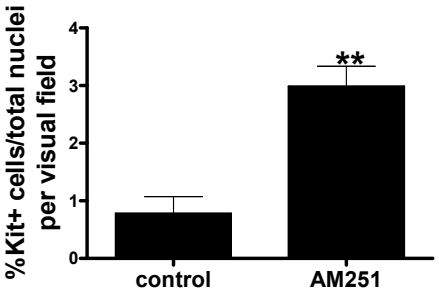

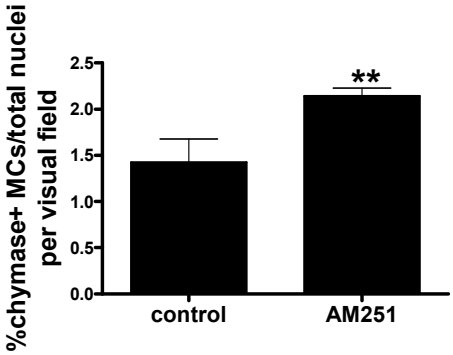

Patient 2.

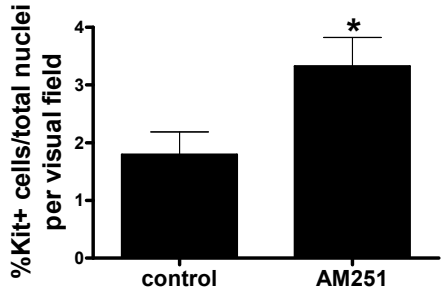

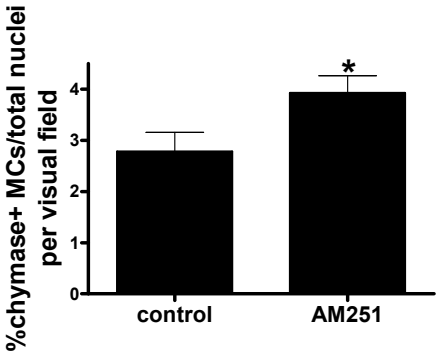

Patient 3.

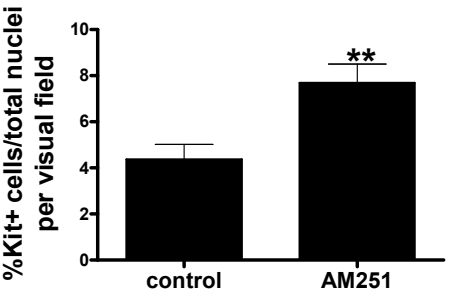

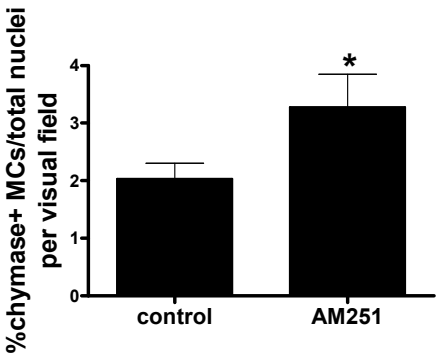

FIG E5.

A

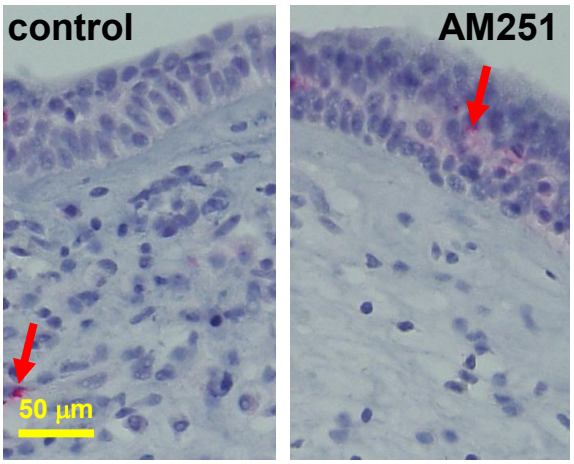
control
AM251
50 µm

B

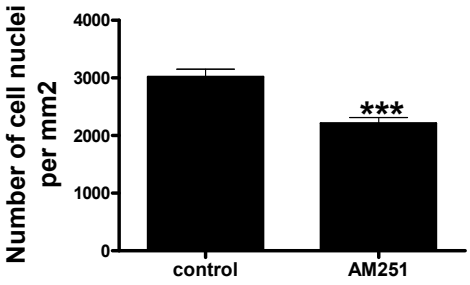
Number of cell nuclei per mm2
4000
3000
2000
1000
0
***
control
AM251

FIG E6.